CALIFORNIA CURRENT INTEGRATED ECOSYSTEM ASSESSMENT (CCIEA) CALIFORNIA CURRENT ECOSYSTEM STATUS REPORT, 2020

A report of the NOAA CCIEA Team to the Pacific Fishery Management Council, March 5, 2020.

Editors: Dr. Chris Harvey (NWFSC), Dr. Toby Garfield (SWFSC), Mr. Greg Williams (PSMFC), and Dr. Nick Tolimieri (NWFSC)
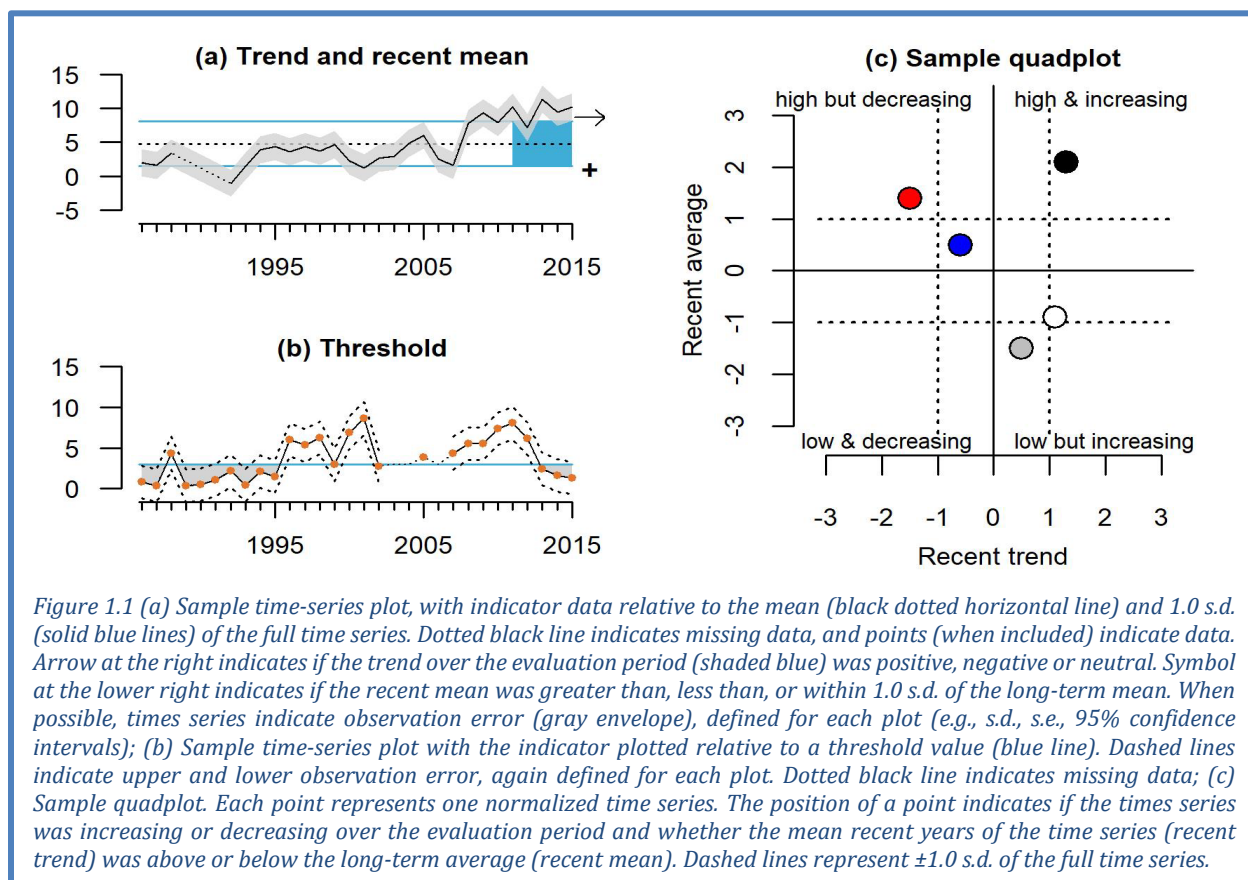
1 INTRODUCTION

Section 1.4 of the 2013 Fishery Ecosystem Plan (FEP) established a reporting process wherein NOAA provides the Pacific Fishery Management Council (Council) with a yearly update on the status of the California Current Ecosystem (CCE), as derived from environmental, biological, economic and social indicators. NOAA's California Current Integrated Ecosystem Assessment (CCIEA) team is responsible for this report. This is our 8th report, with prior reports in 2012 and 2014-2019.

This report summarizes CCE status based on data and analyses that generally run through 2019. Highlights are summarized in Box 1.1. Appendices provide additional information or clarification, as requested by the Council, the Scientific and Statistical Committee (SSC), or other advisory bodies.

Box 1.1: Highlights of this report

- **In 2019, the system experienced weak to neutral El Niño conditions, average to slightly positive Pacific Decadal Oscillation (PDO), and very weak North Pacific circulation**

- **A large marine heatwave emerged in mid 2019, similar in size and intensity to the 2013-2016 "Blob," but it weakened by December, and we do not yet know what effects it had**

- **Several ecological indicators implied average or above-average productivity in 2019:**
  - The copepod community off Oregon was high in cool-water, lipid-rich species in summer
  - Anchovy densities continued to increase along most of the coast
  - Juvenile Chinook and coho salmon catches off Oregon and Washington were average
  - Sea lion pup growth on San Miguel Island was above average

- **However, there was evidence of unfavorable conditions in 2019, particularly off central and northern California:**
  - Krill densities off central and northern California and Oregon were very low
  - Pyrosomes (warm-water tunicates) were abundant in the central CCE
  - Juvenile rockfish, a key forage group in this region, had low abundance
  - Seabird colonies at the Farallon Islands and Año Nuevo had poor production

- **Indicators are consistent with average to below-average salmon returns in 2020**

- **Above-average reports of whale entanglements occurred for the 6th straight year**

- **West Coast fishery landings in 2018 declined 8% relative to 2017; revenue declined 7%**

- **Fishery diversification remains relatively low on average across all vessel classes**

- **We introduce two new indicators in this year's report:**
  - Proportional distribution of commercial fishing revenue among coastal communities
  - Habitat compression, which measures how climate and ocean forcing compresses cooler upwelling habitat along the coast

Throughout this report, most indicator plots follow the formats illustrated in Figure 1.1.

Figure 1.1 (a) Sample time-series plot, with indicator data relative to the mean (black dotted horizontal line) and 1.0 s.d. (solid blue lines) of the full time series. Dotted black line indicates missing data, and points (when included) indicate data. Arrow at the right indicates if the trend over the evaluation period (shaded blue) was positive, negative or neutral. Symbol at the lower right indicates if the recent mean was greater than, less than, or within 1.0 s.d. of the long-term mean. When possible, times series indicate observation error (gray envelope), defined for each plot (e.g., s.d., s.e., 95% confidence intervals); (b) Sample time-series plot with the indicator plotted relative to a threshold value (blue line). Dashed lines indicate upper and lower observation error, again defined for each plot. Dotted black line indicates missing data; (c) Sample quadplot. Each point represents one normalized time series. The position of a point indicates if the times series was increasing or decreasing over the evaluation period and whether the mean recent years of the time series (recent trend) was above or below the long-term average (recent mean). Dashed lines represent ±1.0 s.d. of the full time series.
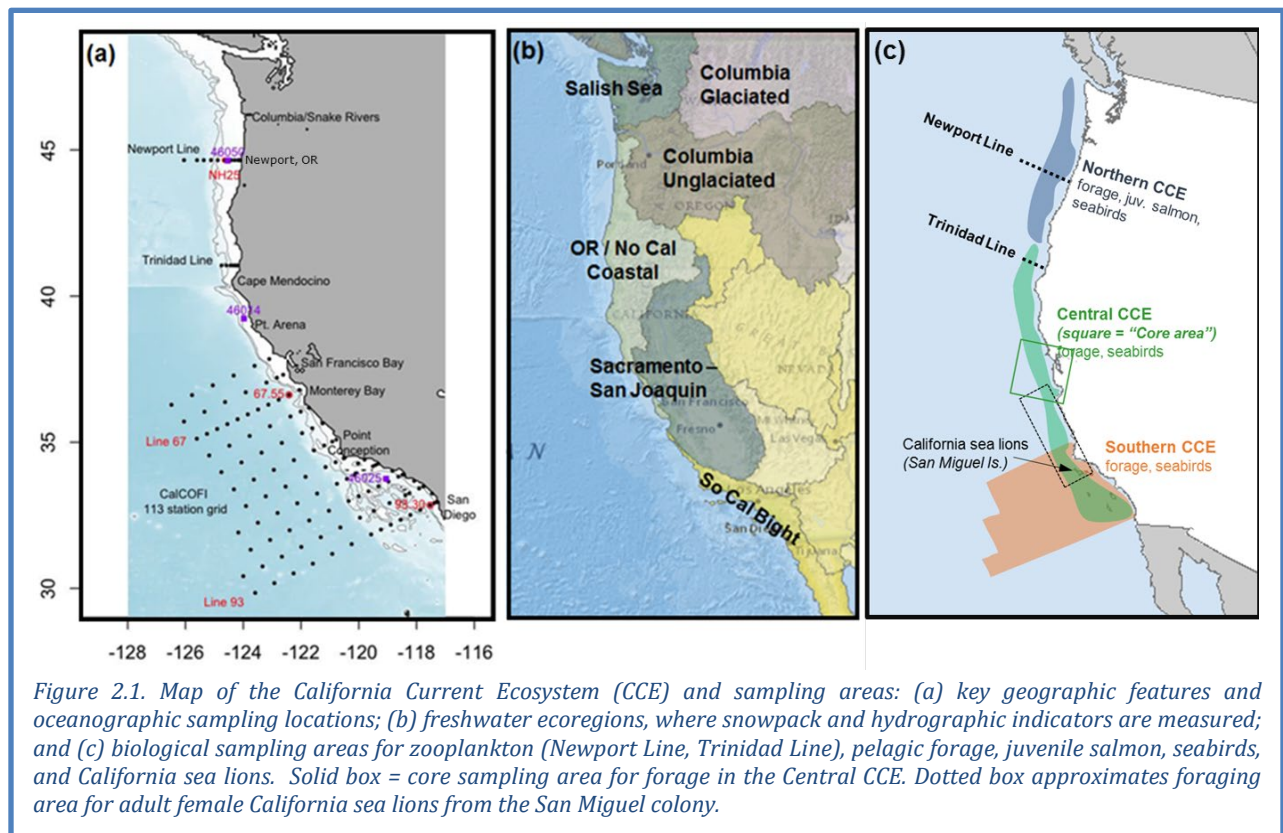
2 SAMPLING LOCATIONS

Figure 2.1a shows the CCE and headlands that define key biogeographic boundaries. We generally consider areas north of Cape Mendocino to be the "Northern CCE," areas between Cape Mendocino and Point Conception the "Central CCE," and areas south of Point Conception the "Southern CCE." Figure 2.1a also shows sampling locations for most regional oceanographic data (Sections 3.2 and 3.3). Key transects are the Newport Line off Oregon, the Trinidad Line off northern California, and the CalCOFI grid further south. This sampling is complemented by basin-scale observations and models.

Freshwater ecoregions in the CCE are shown in Figure 2.1b, and are the basis by which we summarize indicators for snowpack, streamflow and stream temperature (Section 3.5).

Figure 2.1c indicates sampling locations for most biological indicators, including zooplankton (Section 4.1), forage species (Section 4.2), juvenile salmon (Section 4.3), California sea lions (Section 4.6) and seabirds (Section 4.7).

Figure 2.1. Map of the California Current Ecosystem (CCE) and sampling areas: (a) key geographic features and oceanographic sampling locations; (b) freshwater ecoregions, where snowpack and hydrographic indicators are measured; and (c) biological sampling areas for zooplankton (Newport Line, Trinidad Line), pelagic forage, juvenile salmon, seabirds, and California sea lions. Solid box = core sampling area for forage in the Central CCE. Dotted box approximates foraging area for adult female California sea lions from the San Miguel colony.

3 CLIMATE AND OCEAN DRIVERS

The CCE has experienced exceptional ocean warming over the past seven years, due to a mixture of El Niño events and large marine heat waves, including the record heatwave of 2014-2016. This general trend continued in 2019: a weak El Niño event occurred in winter and spring, and a marine heatwave originated in the North Pacific in the summer. El Niño impacts included below-average upwelling during winter and spring 2019 in the central and southern CCE, and above-average spring water temperatures in the south. The heatwave that emerged in the summer was mostly constrained offshore outside of the upwelling zone. It is too early to connect any specific responses in the CCE to this new marine heatwave, but ecosystem impacts can be expected if it reemerges in spring 2020.

The following subsections provide in-depth descriptions of basin-scale, regional-scale, and hydrologic indicators of climate and ocean variability in the CCE.

3.1 BASIN-SCALE INDICATORS

To describe large-scale physical ecosystem states, we report three indices. The Oceanic Niño Index (ONI) describes the equatorial El Niño Southern Oscillation (ENSO). An ONI above 0.5°C indicates El Niño conditions, which usually correspond to lower primary production, weaker upwelling, poleward transport of equatorial waters and species, and more storms to the south in the CCE. An ONI below -0.5°C means La Niña conditions, which usually lead to higher productivity. The Pacific Decadal Oscillation (PDO) describes Northeast Pacific sea surface temperature anomalies (SSTa) that may persist in regimes for many years. Positive PDOs are associated with warmer waters and lower productivity in the CCE, while negative PDOs indicate cooler waters and higher productivity. The North Pacific Gyre Oscillation (NPGO) is a signal of sea surface height, indicating changes in ocean circulation that affect source waters for the CCE. Positive NPGOs are associated with increased equatorward flow and higher surface salinities, nutrients, and chlorophyll-*a*. Negative NPGOs are associated with decreases in such values, less subarctic source water, and lower CCE productivity.

The ONI indicated that a weak El Niño, which began in September 2018, continued through June 2019 (Figure 3.1.1, top). The ONI only recorded a high of 0.9°C (compared to 2.6°C during the strong 2015-2016 El Niño). The ONI was neutral by the end of 2019, and NOAA's Climate Prediction Center forecasts a ~65% chance for neutral ENSO conditions to persist through spring 2020. The PDO has experienced a downward trend from the high positive values of 2013-2016, and was generally neutral in 2019, with values >1.0 only occurring during April-June (Figure 3.1.1, middle). These PDO values were thus above normal, but not nearly as high as in past major El Niño events (1982, 1998, 2016) and the 2013-2016 marine heatwave (the "Blob"). The NPGO in 2019 continued an extended period of negative values, which began in late 2016 (Figure 3.1.1, bottom). Values from October 2017 to June 2019

Figure 3.1.1 Monthly values of the Ocean Nino Index (ONI), Pacific Decadal Oscillation (PDO), and the North Pacific Gyre Oscillation (NPGO) from 1981-2019. Mean and s.d. for 1981-2010 not the full time series. Lines, colors, and symbols are as in Fig. 1.

were among the lowest NPGO values for the whole record since 1950. Thus, the three basin-scale indices provide a mixed signal of general conditions in the CCE: the ONI and NPGO were consistent with lower productivity, while the PDO was neutral, implying average productivity. Seasonal values for basin-scale indices are in Appendix D.1.
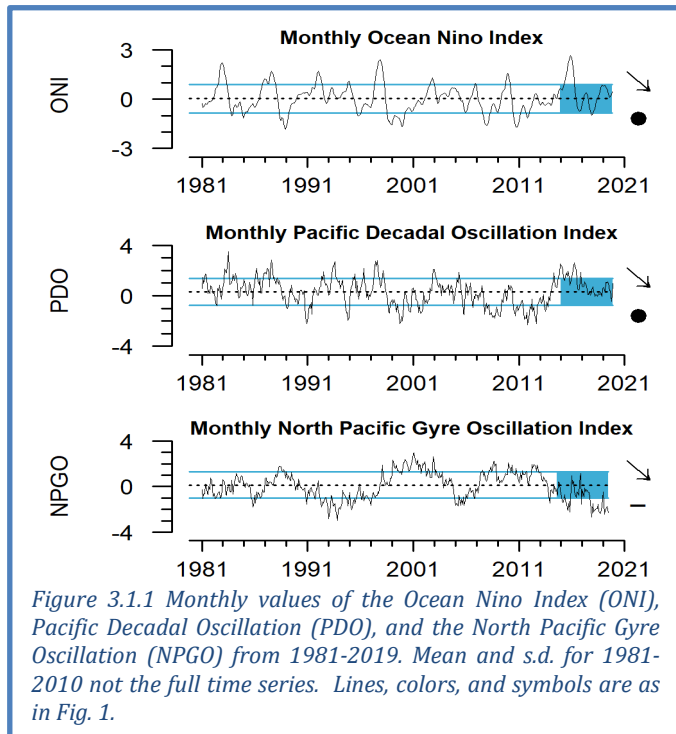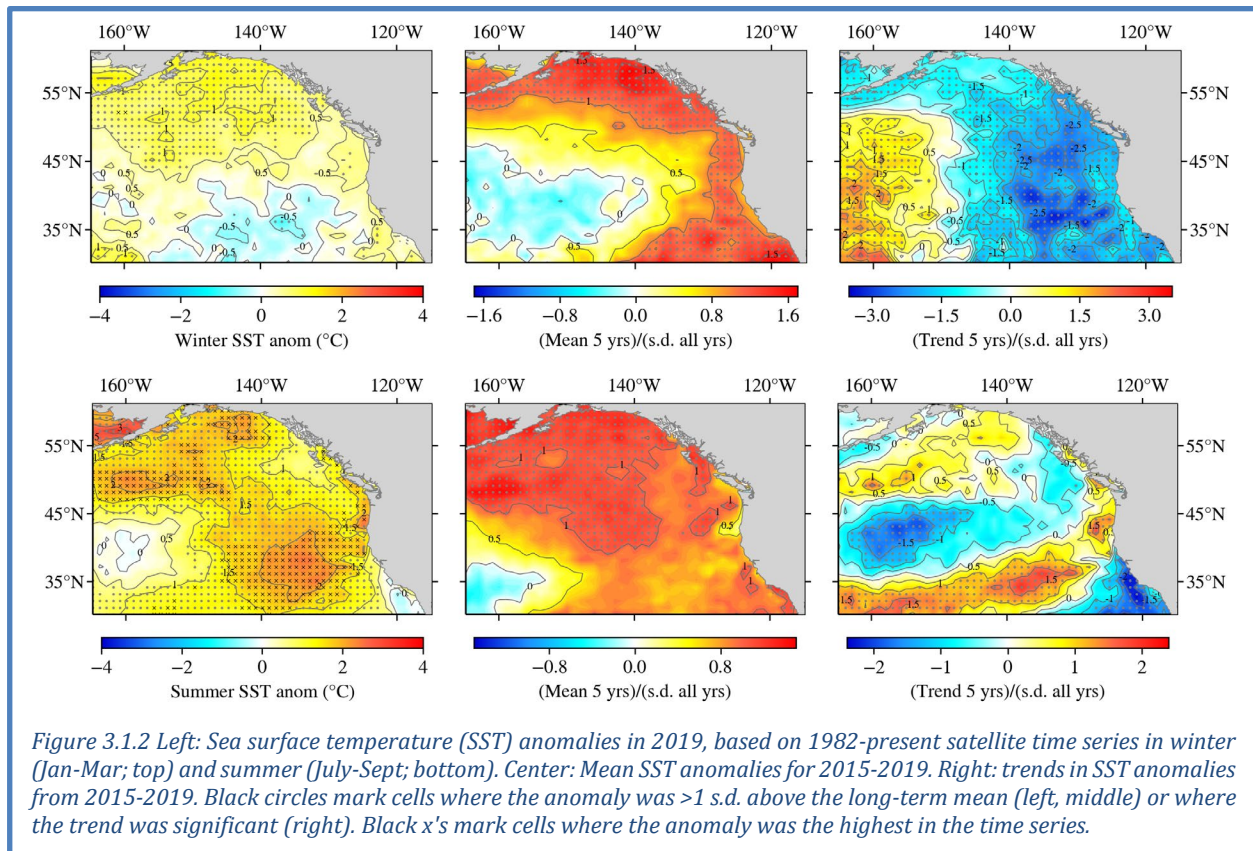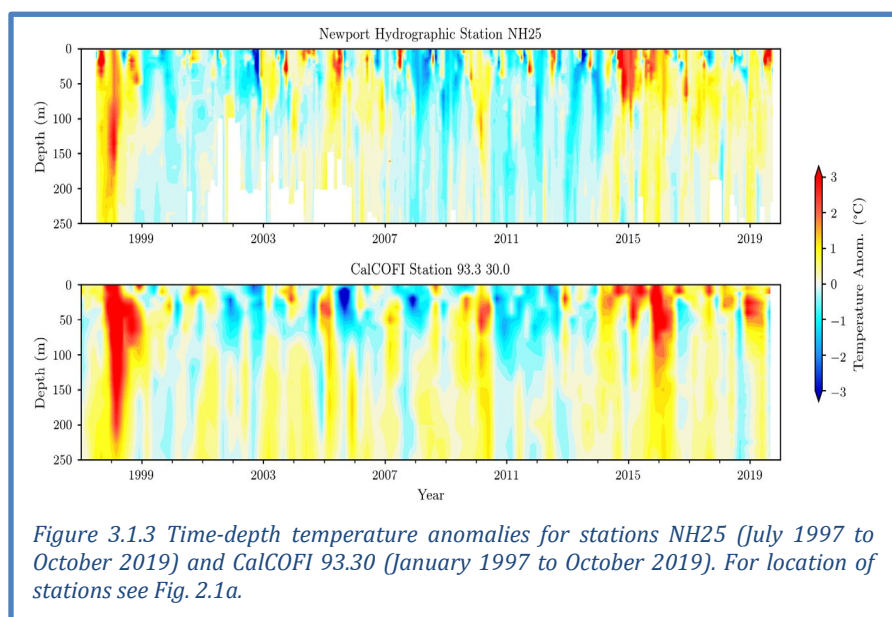
Bering Sea and Gulf of Alaska warming extended into the northeast Pacific during 2019 (Figure 3.1.2, left). Positive SST anomalies increased and the spatial extent of warming expanded over the course of 2019, with the warmest anomalies and greatest spatial extent occurring in summer and fall. Winter SST measurements were ~0.5°C warmer than average along the coast, while warming anomalies were 0.5 to 1.0°C above long-term mean for most cells above 48°N (Figure 3.1.2, upper left). Summer 2019 anomalies were more extreme, representing the development of another marine heatwave (see Section 7.2 for additional detail). A quarter of the grid cells had the highest recorded temperature anomalies since 1982 (Figure 3.1.2, lower left). Along the West Coast, summer 2019 anomalies ≥1 SD occurred north of Monterey Bay, while coastal anomalies to the south were neutral.

Five-year average SST anomalies demonstrate the extended warming that the CCE has experienced for many years. The 5-year average winter SSTa in the CCE was generally ≥1 SD above average, with slightly cooler but still positive anomalies closer to shore (Figure 3.1.2, upper middle). The 5-year average summer SSTa was positive for most of the Northeast Pacific, again with some slightly cooler warm anomalies in the coastal CCE (Figure 3.1.2, lower middle). Trends in winter SSTa over the last 5 years have been negative (Figure 3.1.2, upper right), due to recent years being cooler than the winters associated with the 2013-2016 marine heatwave. Summer 5-year trends along the coast were positive north of Cape Mendocino and negative to the south (Figure 3.1.2, lower right). Summer trends were mixed in the rest of the Northeast Pacific.

Figure 3.1.2 Left: Sea surface temperature (SST) anomalies in 2019, based on 1982-present satellite time series in winter (Jan-Mar; top) and summer (July-Sept; bottom). Center: Mean SST anomalies for 2015-2019. Right: trends in SST anomalies from 2015-2019. Black circles mark cells where the anomaly was >1 s.d. above the long-term mean (left, middle) or where the trend was significant (right). Black x's mark cells where the anomaly was the highest in the time series.

Depth profiles of temperatures off Newport, Oregon and San Diego show that the warming in 2019 was mostly confined to surface waters, and that seasonal patterns differed in the north and south. At NH25 off Newport, temperature anomalies through spring 2019 were small and variable in sign, but then rose to strongly positive (>1°C) anomalies during the late summer and early fall 2019, constrained to the upper 25 m of the water column (Figure 3.1.3, top). The subsurface water off Newport remained warmer than normal into the fall. CalCOFI station 93.30 off San Diego had large

positive anomalies (>1°C) in winter and spring 2019 in the upper 50 m depth layer (Figure 3.1.3, bottom). By summer 2019, most of the water column had cooled to negative anomalies, though the upper 10 m still had large positive anomalies. Figure 3.1.3 also shows how persistent the warm anomalies at depth have been since 2014 at both stations, and the relative dominance of warm water at depth off San Diego since at least 1997.

Figure 3.1.3 Time-depth temperature anomalies for stations NH25 (July 1997 to October 2019) and CalCOFI 93.30 (January 1997 to October 2019). For location of stations see Fig. 2.1a.

5

3.2 REGIONAL CLIMATE AND OCEAN INDICATORS

Upwelling in the CCE occurs when equatorward winds move deep, cold, nutrient-rich water to the surface layer, fueling the high seasonal production in the CCE food web. On average, upwelling peaks in late April near San Diego, mid June off Point Arena in Central California, and late July off Newport, Oregon. Nutrient delivery by upwelling also varies in space: vertical flux of nitrate at Point Arena is an order of magnitude greater than at Newport or San Diego. Jacox et al. (2018) developed models to estimate the vertical transport of water (Cumulative Upwelling Transport Index; CUTI) and nitrate flux (Biologically Effective Upwelling Transport Index; BEUTI) for the CCE.

In 2019, upwelling volume (CUTI) at 45°N during winter and spring was slightly above the long-term mean, while at 33°N and 39°N CUTI values varied around or below the mean (Figure 3.2.1, left). Nitrate fluxes (BEUTI) in winter and spring 2019 were mostly average coastwide, except for some below-average periods in winter and spring at 39°N (Figure 3.2.1, right). In summer, CUTI was generally average or below-average in the north, but average to above-average in the central and southern regions. However, nitrate fluxes in the summer were average to above-average in all regions (Figure 3.2.1, right).
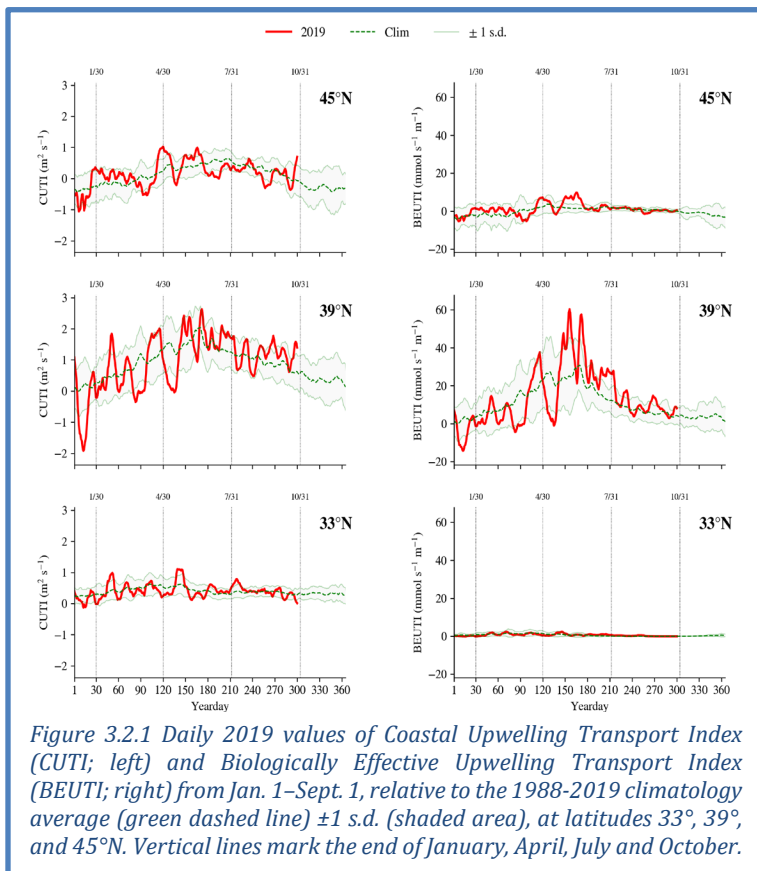

Figure 3.2.1 Daily 2019 values of Coastal Upwelling Transport Index (CUTI; left) and Biologically Effective Upwelling Transport Index (BEUTI; right) from Jan. 1–Sept. 1, relative to the 1988-2019 climatology average (green dashed line) ±1 s.d. (shaded area), at latitudes 33°, 39°, and 45°N. Vertical lines mark the end of January, April, July and October.

3.3 HYPOXIA AND OCEAN ACIDIFICATION

Dissolved oxygen (DO) is dependent on processes such as currents, upwelling, air-sea exchange, primary production, and respiration. Low DO can compress habitat and cause stress or die-offs for sensitive species. Waters with DO levels <1.4 ml/L (2 mg/L) are considered hypoxic.

Near-bottom DO measurements at station NH05 (5 nautical miles off of Newport, Oregon) fell below the hypoxia threshold in August 2019 but rebounded by September (Figure 3.3.1, top). This was a similar intensity of hypoxia to 2018, although the 2018
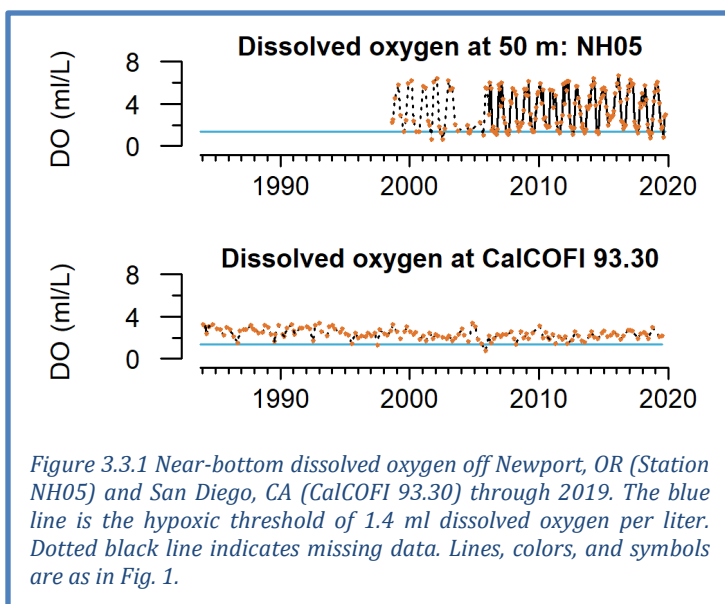

Figure 3.3.1 Near-bottom dissolved oxygen off Newport, OR (Station NH05) and San Diego, CA (CalCOFI 93.30) through 2019. The blue line is the hypoxic threshold of 1.4 ml dissolved oxygen per liter. Dotted black line indicates missing data. Lines, colors, and symbols are as in Fig. 1.
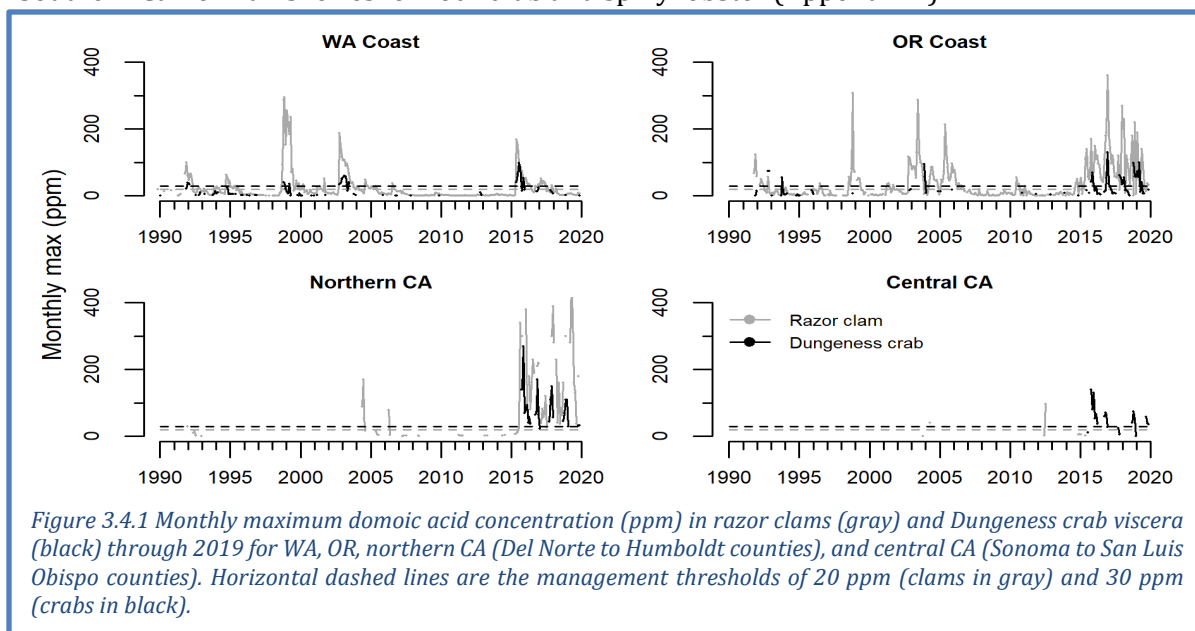
hypoxic period off Newport lasted from June to September. Off San Diego at CalCOFI station 93.30, near-bottom DO was above the hypoxia threshold in spring and summer cruises (Figure 3.3.1, bottom), and DO values throughout the CalCOFI region were close to average (Appendix D.3). DO maps and time series for additional stations off Oregon and Southern California are in Appendix D.3.

Ocean acidification, caused by increased levels of atmospheric CO_2, lowers pH and carbonate in seawater and can be stressful to shell-forming organisms and other species (Chan et al. 2008, Feely et al. 2008, Bednaršek et al. 2020). Off Newport Oregon, levels of aragonite (a form of calcium carbonate) near the seafloor in 2019 were similar to 2018, and lower than in the anomalous years of 2014–2015. More of the water column was above the saturation threshold in 2019 than in 2017 or 2018. For space considerations, we present ocean acidification data in Appendix D.3.

3.4 HARMFUL ALGAL BLOOMS

Blooms of the diatom *Pseudo-nitzschia* can increase concentrations of the toxin domoic acid in coastal waters, creating harmful algal blooms (HABs). Domoic acid can enter the food web via filter feeders like razor clams. Because domoic acid can cause amnesic shellfish poisoning in humans, fisheries for razor clams, Dungeness crab and other species are closed when concentrations exceed regulatory thresholds for human consumption. Extremely toxic HABs of *Pseudo-nitzschia* may coincide with warm events in the CCE, such as the 2014-2016 marine heatwave (Appendix E).

In 2019, elevated levels of domoic acid occurred in razor clams and Dungeness crabs in parts of Oregon and California, while low levels of domoic acid were detected in Washington razor clams and Dungeness crabs (Figure 3.4.1). Domoic acid levels extended years-long closures of razor clam fisheries in southern Oregon and northern California, and closed all of Oregon razor clam fisheries in December 2019 (Appendix E). Domoic acid contributed to delayed openings of Dungeness crab fisheries in 2019 in southern Oregon and in parts of central California, and northern California rock crab fisheries have been closed in some areas since 2015 (Appendix E). In contrast, there were no domoic acid-related razor clam or Dungeness crab closures in Washington in 2019 (Figure 3.4.1), or in Southern California fisheries for rock crab and spiny lobster (Appendix E).

Figure 3.4.1 Monthly maximum domoic acid concentration (ppm) in razor clams (gray) and Dungeness crab viscera (black) through 2019 for WA, OR, northern CA (Del Norte to Humboldt counties), and central CA (Sonoma to San Luis Obispo counties). Horizontal dashed lines are the management thresholds of 20 ppm (clams in gray) and 30 ppm (crabs in black).

3.5 HYDROLOGIC INDICATORS

Freshwater conditions are critical for salmon populations and West Coast estuaries. Hydrologic
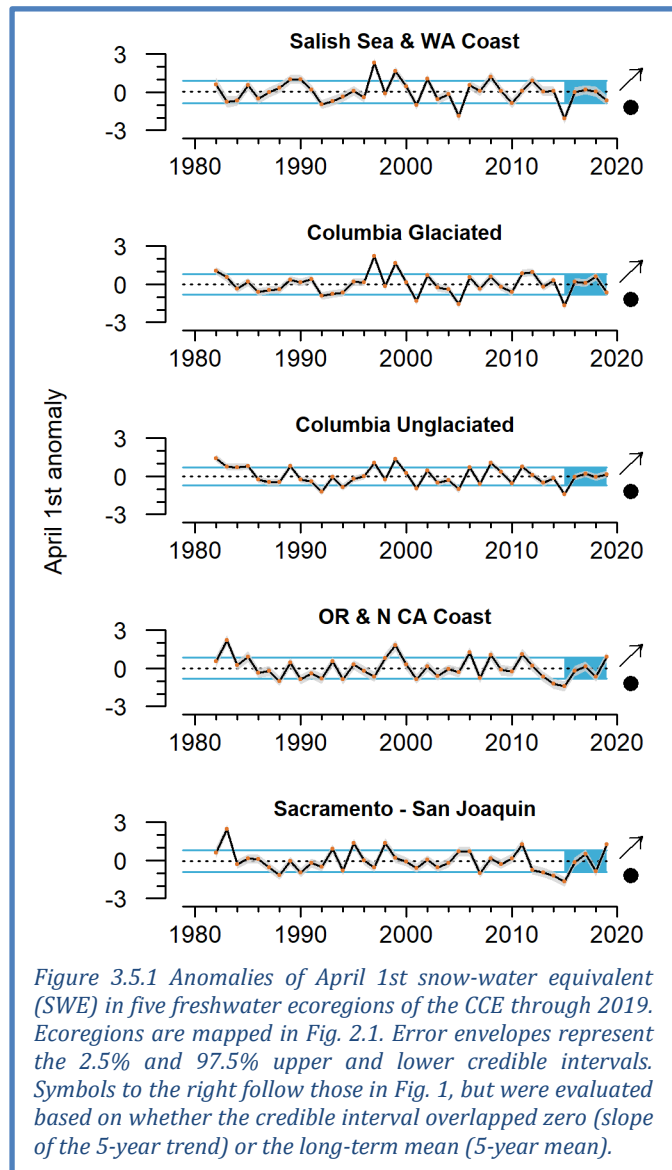
indicators presented here are snowpack, streamflow and stream temperature, summarized by ecoregion (Figure 2.1b) or by salmon evolutionarily significant units (ESUs, Waples 1995). Snow-water equivalent (SWE) is the water content in snowpack, which provides cool freshwater in the spring, summer and fall months. Maximum streamflow in winter and spring is important for habitat formation and removal of parasites, but extreme discharge relative to historic averages can scour salmon nests (redds). Below-average minimum streamflow in summer and fall can restrict habitat for juvenile salmon and migrating adults. High summer temperatures can impair physiology and cause mortality.
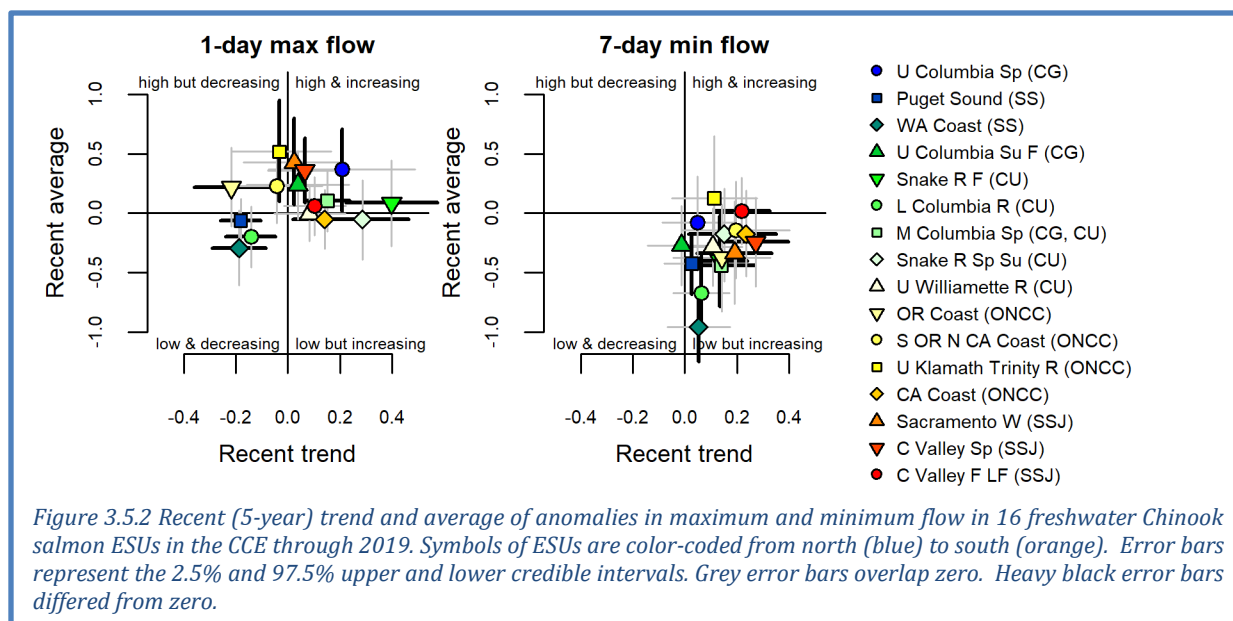
In 2019, SWE in the two northern regions (Salish Sea/WA Coast and Columbia River Glaciated) declined relative to 2018 (Figure 3.5.1), and drought conditions were declared in parts of Washington. In contrast, SWE was above average in 2019 for Sacramento/San Joaquin and coastal California and Oregon. All regions have increasing trends, due to rebounds since the extreme lows of 2015 (Figure 3.5.1).

As of February 1st, SWE in 2020 is mixed. Most stations are average to below average, although portions of Washington, eastern Oregon, Idaho, and parts of interior northern California are above average (Appendix F). Because SWE values typically do not peak until early spring, the official measure of SWE will be on April 1, 2020.

Minimum streamflows were consistent with SWE, with generally increasing trends since lows in 2015, particularly in central and southern ecoregions (Appendix F). Maximum flows have experienced increasing 5-year trends in the Southern California Bight, Sacramento/San Joaquin, and Unglaciated Columbia Basin, but decreasing trends in the Salish Sea/WA Coast ecoregion (Appendix F). Maximum August stream temperatures have not exhibited strong trends except for the Salish Sea/WA Coast ecoregion, where they have increased over the past 5 years (Appendix F).

Figure 3.5.1 Anomalies of April 1st snow-water equivalent (SWE) in five freshwater ecoregions of the CCE through 2019. Ecoregions are mapped in Fig. 2.1. Error envelopes represent the 2.5% and 97.5% upper and lower credible intervals. Symbols to the right follow those in Fig. 1, but were evaluated based on whether the credible interval overlapped zero (slope of the 5-year trend) or the long-term mean (5-year mean).

We also summarized streamflows at the finer scale of individual Chinook salmon ESUs. These results are presented in quad plots, showing flow anomalies and 95% credible intervals to indicate ESUs with significant short-term trends or recent averages that differ from long-term means. With the exception of Salish Sea, northern coastal sites and the Lower Columbia, maximum flows have generally increased since 2015 (Figure 3.5.2, left; Appendix F). Because high rates of winter flow are generally beneficial for juvenile salmon in inland regions but detrimental to northern coastal populations, these trends suggest improving flow conditions during egg incubation across much of

Figure 3.5.2 Recent (5-year) trend and average of anomalies in maximum and minimum flow in 16 freshwater Chinook salmon ESUs in the CCE through 2019. Symbols of ESUs are color-coded from north (blue) to south (orange). Error bars represent the 2.5% and 97.5% upper and lower credible intervals. Grey error bars overlap zero. Heavy black error bars differed from zero.

the CCE. Minimum flows were generally below average but increasing since the very low flows of 2015, with the strongest short-term increases in southern and inland ESUs (Figure 3.5.2, right; Appendix F). ESUs in the northwest tended to be the furthest below average, including three Columbia Basin ESUs, Puget Sound, and the Washington Coast.

4 FOCAL COMPONENTS OF ECOLOGICAL INTEGRITY

The CCIEA team examines many indicators related to the abundance and condition of key species and the dynamics of ecological interactions and community structure. Many CCE species and processes respond very quickly to changes in ocean and climate drivers, while other responses may not manifest for many years. These dynamics are challenging to predict. In 2019, ecological indicators implied average to above-average productivity in the northern and southern portions of the CCE, but average to below-average conditions in the central CCE. The marine heatwave that developed in mid 2019 may have affected portions of the system later in the year, but we have relatively little data to demonstrate impacts at this time.

4.1 COPEPOD BIOMASS ANOMALIES AND KRILL SIZE

Copepod biomass anomalies represent variation for northern copepods, which are cold-water species rich in wax esters and fatty acids, and southern copepods, which are smaller and have lower fat content and nutritional quality. In summer, northern copepods usually dominate the zooplankton community along the Newport Line (Figure 2.1a,c), while southern copepods dominate in winter. Positive values of northern copepods correlate with stronger returns of Chinook salmon to Bonneville Dam and coho salmon to coastal Oregon (Peterson et al. 2014). El Niño events and positive PDO regimes can increase southern copepods (Keister et al. 2011, Fisher et al. 2015).
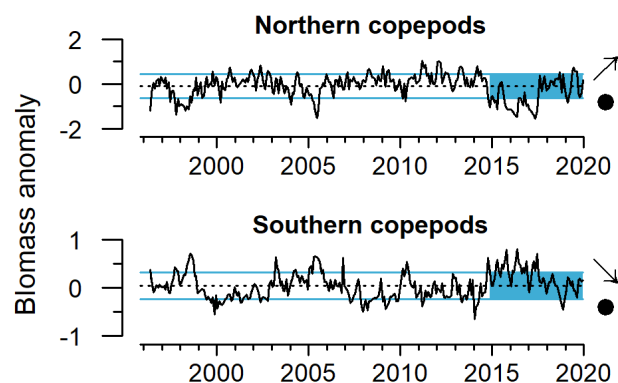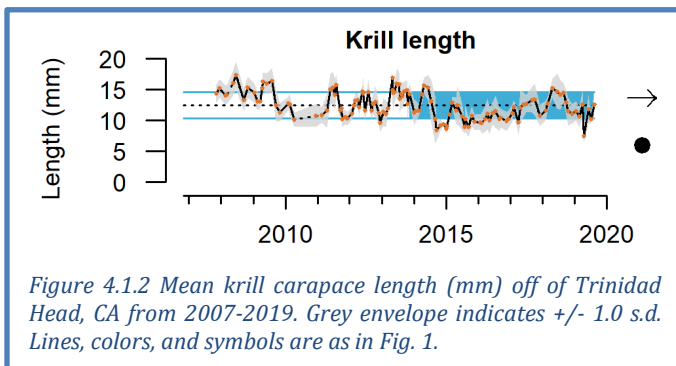

Figure 4.1.1 Monthly northern and southern copepod biomass anomalies from station NH05, 1996-2019. Lines, colors and symbols are as in Fig. 1.

In 2019, northern copepods continued an overall increasing trend since the extreme lows during the 2014-2016 heatwave. They were ~1 s.d. above the mean in spring-summer 2019, but declined by September (Figure 4.1.1, top). The spring-summer anomaly was among the highest of the time series, despite weak El Niño conditions. However, the northern copepods appeared relatively late and declined relatively early, resulting in a short duration of the northern copepod community. Southern copepods were near-average for most of 2019, continuing a decline since the heatwave (Figure 4.1.1, bottom). These values suggest average to above-average feeding conditions for pelagic fishes off central Oregon in 2019, with the best copepod ratios in the summer.

Krill are among the most important prey for fishes, mammals and seabirds in the CCE. The key species *Euphausia pacifica* has been sampled multiple times per season off of Trinidad Head (Figure 2.1a,c) since late 2007. Mean length of adult *E. pacifica* is an indicator of krill as a resource for predators. *E. pacifica* length cycles from short individuals in winter that grow into longer individuals by summer. *E. pacifica* lengths were very low during the first half of 2019

Figure 4.1.2 Mean krill carapace length (mm) off of Trinidad Head, CA from 2007-2019. Grey envelope indicates +/- 1.0 s.d. Lines, colors, and symbols are as in Fig. 1.
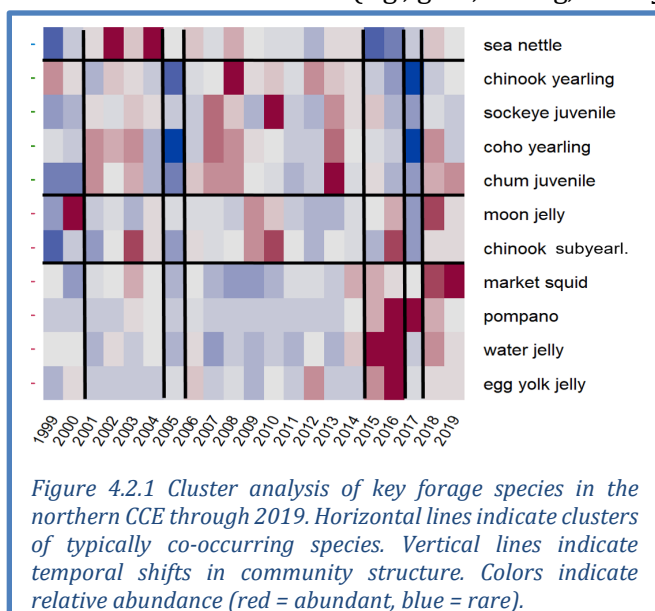
(Figure 4.1.2), coincident with El Niño conditions during the 2018-2019 winter. This marked a decrease relative to 2018, when lengths were generally above average and consistent with conditions associated with typical seasonal upwelling. Krill lengths had been gradually increasing after poor growth at the onset of the 2014-2016 heatwave. The 2019 results suggest that krill production in the northern CCE continues to be impacted by ocean forcing such as recent warming and the weak NPGO.

4.2 REGIONAL FORAGE AVAILABILITY

The CCE forage community is a diverse portfolio of species and life history stages, varying in behavior, energy content, and availability to predators. The species summarized below represent a substantial portion of the available forage in the CCE. *We consider these regional indices of relative forage availability and variability, not indices of stock biomass of coastal pelagic species (CPS).*

The regional surveys that produce CCE forage data use different methods (e.g., gear, timing, survey design), which makes regional comparisons difficult. We use cluster analysis (Thompson et al. 2019a) to identify and compare regional shifts in forage composition. Co-occuring species cluster on the y-axis, and yearly abundance estimates are indicated by color (red = abundant, blue = rare); temporal shifts in forage composition are marked by vertical lines. Related time series are in Appendix G.

Northern CCE: The northern CCE survey off Washington and Oregon (Figure 2.1c) targets juvenile salmon in surface waters, but also samples surface-oriented fishes, squid and jellies. This forage assembly has had several recent shifts since the onset of the 2014-2016 marine heatwave (Figure 4.2.1). Since the most recent shift prior to 2018, market squid,

Figure 4.2.1 Cluster analysis of key forage species in the northern CCE through 2019. Horizontal lines indicate clusters of typically co-occurring species. Vertical lines indicate temporal shifts in community structure. Colors indicate relative abundance (red = abundant, blue = rare).

juvenile coho and chum salmon, and several jellies have been abundant. Some species that were abundant during the previous marine heatwave (e.g., pompano, water jelly, egg yolk jelly) were less abundant in 2018-2019. Related surveys off Oregon and southern Washington indicated that krill abundance was very low in 2019, and has been for several years (Appendix G.1).

Central CCE: Data presented here are from the "Core area" of a survey (Figure 2.1c) that targets pelagic juvenile rockfishes, but also samples other pelagic species. Since 2018, this forage base has been dominated by anchovy, with adult anchovy more abundant in 2019 than any previous year surveyed (Figure 4.2.2; Appendix G.2). Adult sardine in 2019 were the most abundant in a decade, though not as abundant as in the 2000s. Market squid remained abundant, as did several myctophids. However, juvenile rockfish, hake, and flatfish, which had been abundant from 2013-2017, have declined to low abundances in the past two years. A concerning sign was that krill catches were the lowest of the time series (Appendix G.2).

Southern CCE: Forage data for the Southern CCE (Figure 2.1c) come from CalCOFI larval fish surveys. The larval biomass of forage species is assumed to correlate with regional abundance of adult forage species. The southern forage assemblage has experienced 6 substantial shifts from 1998-2019. Since 2017, the community has been characterized by abundant larval anchovy and warm-water

Figure 4.2.2 Cluster analysis of key forage species in the central CCE through 2019. Lines and colors are as in Figure 4.2.1.

Figure 4.2.3 Cluster analysis of key forage species in the southern CCE through 2019. Lines and colors are as in Figure 4.2.1.

mesopelagic fishes (Figure 4.2.3; Appendix G.3). Larval anchovy abundance was the greatest it has been in the history of the CalCOFI time series. Larvae of other forage species were near long-term averages (e.g., rockfish, English sole, market squid) or below average (cool water mesopelagics, sardine, mackerels, sanddabs).

Pyrosomes, a warm-water pelagic tunicate, have been abundant in different regions of the CCE since the onset of warming in 2014. They cause fouling of fishing gear and have likely affected food web dynamics. Pyrosome distribution shifted considerably in 2019: after reaching extreme densities off of Washington and Oregon in 2017 and 2018, they were nearly absent in 2019. In contrast, pyrosome densities off of California were similar to densities from 2015-2016 (Miller et al. 2019; Appendix G.4).
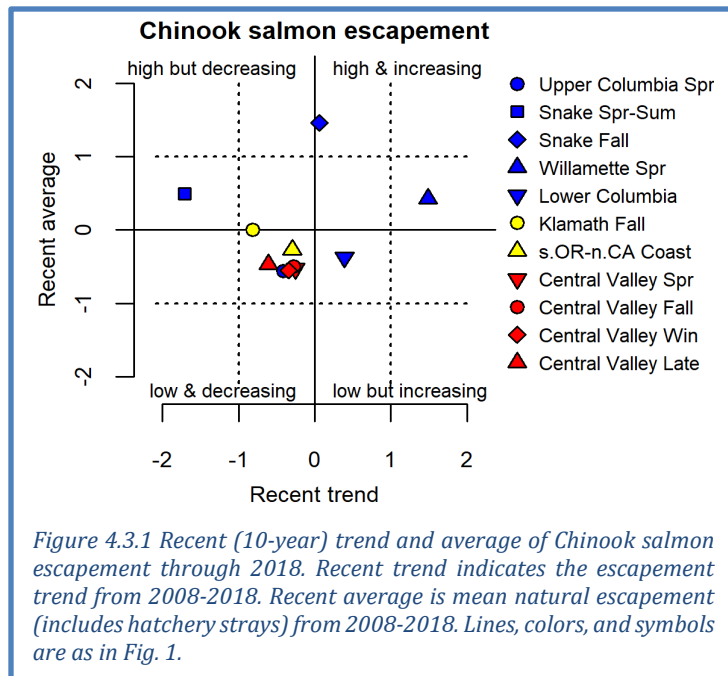
4.3 SALMON

Chinook salmon escapement: For indicators of the abundance of naturally spawning Chinook salmon, we examine trends in natural spawning escapement from different populations to compare status
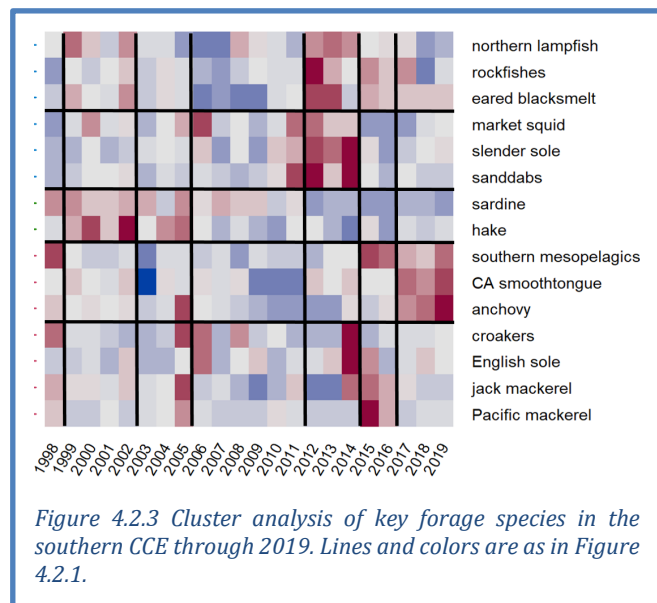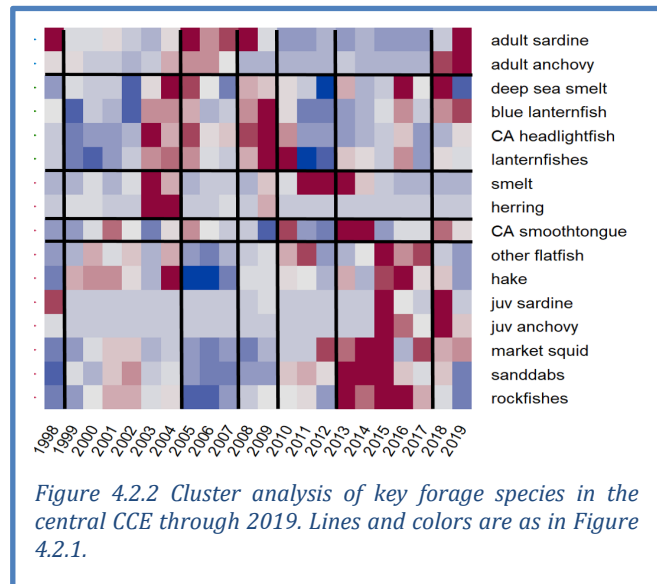
and coherency in production dynamics across their range. We summarize escapement trends in quad plots; time series are shown in Appendix H. Most escapement data are updated through 2018.

Escapements of California Chinook salmon ESUs over the last decade were within 1 s.d. of long-term means (Figure 4.3.1), though 2018 escapements were among the lowest on record in several ESUs, particularly in the Central Valley (Appendix H.1). California ESUs had neutral trends over the last decade, though some sharp declines occurred ~5 years ago (Appendix H.1). In the Northwest, most mean escapements in the past decade were within 1 s.d. of average; the exception was above-average Snake River Fall Chinook

Figure 4.3.1 Recent (10-year) trend and average of Chinook salmon escapement through 2018. Recent trend indicates the escapement trend from 2008-2018. Recent average is mean natural escapement (includes hatchery strays) from 2008-2018. Lines, colors, and symbols are as in Fig. 1.

escapements, due to relatively large escapements from 2009 to 2016 (Appendix H.2). Escapement trends for Northwest stocks over the past decade were mostly neutral, but Willamette Spring Chinook had a positive trend while Snake River Spring-Summer Chinook had a negative trend.

Juvenile salmon abundance: Annual catches of juvenile coho and Chinook salmon from surveys during June in the Northern CCE (Figure 2.1c) can serve as indicators of salmon survival during their first few weeks at sea. In 2019, catches of subyearling Chinook, yearling Chinook, and yearling coho salmon were all very close to long-term averages (Figure 4.3.2). The 5-year catch trends were neutral but variable for all groups. Juvenile salmon captured off Oregon and Washington in 2019 generally appeared to be in good condition.

Long-term associations between oceanographic conditions, food web structure, and salmon productivity (Burke et al. 2013, Peterson et al. 2014) support projections of returns of Chinook salmon to

Figure 4.3.2 At sea juvenile salmon catch (Log₁₀(no/(km + 1))) from 1998 to 2019 for Chinook and coho salmon. Lines, colors, and symbols are as in Fig. 1.

Bonneville Dam and smolt-to-adult survival of Oregon Coast coho salmon. The suite of indicators is depicted in the "stoplight chart" in Table 4.3.1, and includes many indicators shown elsewhere in this report (PDO, ONI, SSTa, deep temperature, copepods, juvenile salmon catch). Indicators for 2020 salmon returns reflect a range of conditions, from poor in smolt years 2016 and 2017 to more mixed conditions in smolt year 2018. Taken as a whole, these indicators are consistent with average returns of Chinook salmon to the Columbia River in 2020, relative to the past two decades. Conditions in smolt year 2019 were a mix of good, intermediate and poor conditions, consistent with average to
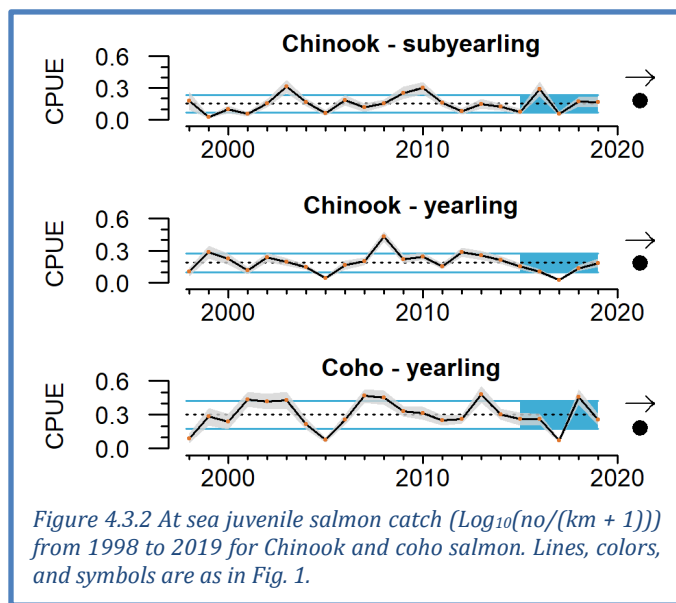
Table 4.3.2 "Stoplight" table of basin-scale and local-regional conditions for smolt years 2016-2019 and projected adult returns in 2020 for coho and Chinook salmon that inhabit coastal Oregon and Washington waters in their marine phase. Green/circle = "good," yellow/square = "intermediate," and red/diamond = "poor," relative to long-term time series.

Scale of indicators	Smolt year 2016	2017	2018	2019	Adult return outlook Coho, 2020	Chinook, 2020
Basin-scale						
PDO (May-Sept)	red diamond	yellow square	yellow square	red diamond	red diamond	yellow square
ONI (Jan-Jun)	red diamond	yellow square	green circle	red diamond	red diamond	green circle
Local and regional						
SST anomalies	red diamond	yellow square	yellow square	red diamond	red diamond	yellow square
Deep water temp	yellow square	red diamond	red diamond	red diamond	red diamond	red diamond
Deep water salinity	yellow square	yellow square	green circle	red diamond	red diamond	green circle
Copepod biodiversity	red diamond	red diamond	yellow square	yellow square	yellow square	yellow square
Northern copepod anomaly	red diamond	red diamond	yellow square	green circle	green circle	yellow square
Biological spring transition	red diamond	red diamond	yellow square	yellow square	yellow square	yellow square
Winter ichthyoplankton biomass	yellow square	yellow square	yellow square	red diamond	red diamond	yellow square
Winter ichthyoplankton community	red diamond	red diamond	red diamond	red diamond	red diamond	red diamond
Juvenile Chinook catch (Jun)	red diamond	red diamond	yellow square	yellow square	yellow square	yellow square
Juvenile coho catch (Jun)	yellow square	red diamond	green circle	yellow square	yellow square	yellow square

below-average returns of coho to the Oregon coast in 2020. A related quantitative model indicates a probability of modest increases in returns of Fall Chinook in the Columbia River relative to 2018 and 2019, but returns of Spring Chinook that are similar to 2017-2019 (Appendix H.3).

At the request of several Council groups, we are working to develop similar indicator-based outlooks for returns of Chinook salmon in California. As a first iteration, a recent paper by Friedman et al. (2019) found that returns of naturally produced Central Valley fall run Chinook salmon were correlated with spawning escapement of parent generations, egg incubation temperature between October and December at Red Bluff Diversion Dam (Sacramento River), median flow in the Sacramento River in the February after fry emergence, and a marine predation index based on the abundance of common murres at Southeast Farallon Island. For fall Chinook salmon cohorts returning to the Central Valley in 2020, these four indicators imply relatively low returns for age-3 Chinook salmon, the dominant age group for this system (Table 4.3.2). Age-3 fish returning in 2020

Table 4.3.1 Table of conditions for naturally produced Central Valley fall run Chinook salmon returning in 2020, from spawning years 2016-2018. Indicators reflect each cohort's parent generation escapement, egg incubation temperature, flow during juvenile stream residence, and seabird predation in the early marine phase. Heavy outline and boldfaced type indicates age-3 Chinook salmon, the dominant age class returning to the Central Valley.
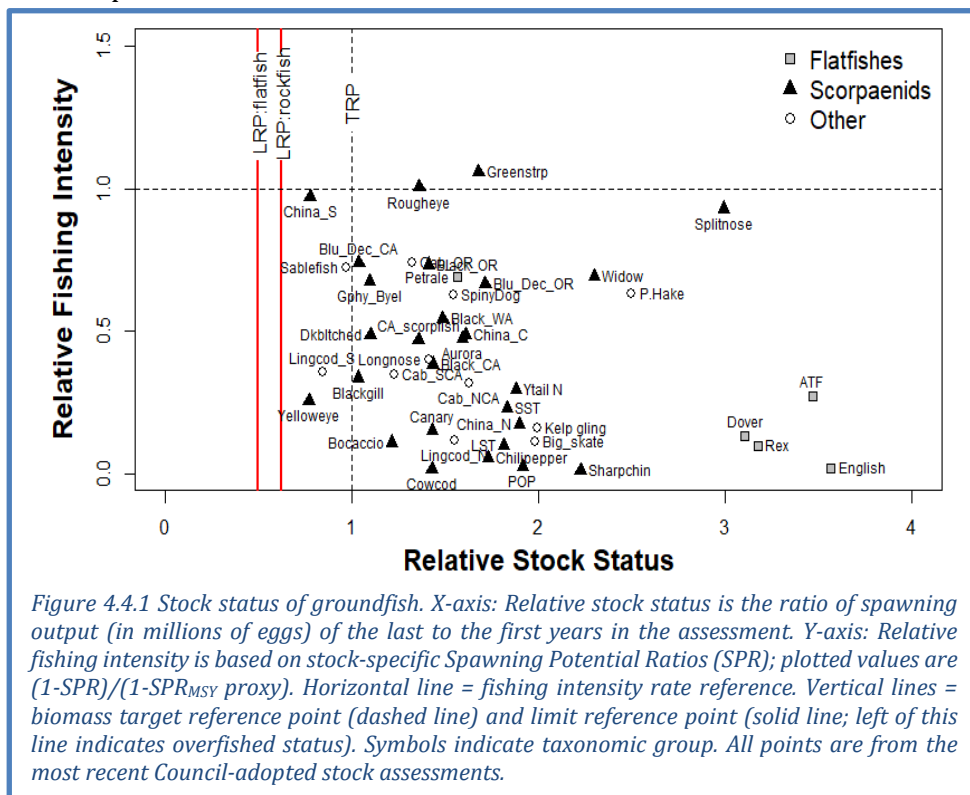
Spawning Escapement (t=0)	Incubation Temperature (Oct-Dec t=0)	February Median Flow (t+1)	Seabird Marine Predation Index (t+1)	Chinook Age in Fall 2020
2016: 56,000 (low)	11.8°C (poor)	48,200 cfs (very high)	Near average	4
2017: 18,000 (very low)	**11.8°C (poor)**	**5,525 cfs (very low)**	**Near average**	**3**
2018: 72,000 (low)	11.7°C (poor)	21,700 cfs (high)	Near Average	2

were the progeny of a very low escapement year (2017), experienced poor incubation temperature in the 2017-2018 winter, and very low streamflow in early 2018, likely coupled with typical predation pressure as they went to sea later in 2018. Age-4 fish (produced in 2016) and age-2 jacks (2018) have somewhat more mixed signals thanks to better juvenile flow regimes.

4.4 GROUNDFISH STOCK ABUNDANCE

The CCIEA team regularly presents the status of groundfish biomass and fishing pressure based on the most recent stock assessments. This year's report includes updated information for 10 stocks (big and longnose skates, 3 cabezon substocks, Pacific hake, sablefish, cowcod and combined gopher/black-and-yellow rockfish), plus many catch-only projections. This leaves splitnose rockfish as the only full assessment done prior to 2010.

All assessed stock biomasses are above limit reference points (LRPs); thus, no assessed stocks were considered overfished (Figure 4.4.1, x-axis). Yelloweye rockfish is still rebuilding toward its target reference point (TRP), but cowcod is now above its TRP. Only two stocks (rougheye and greenstriped rockfish) are above the proxy for overfishing (Figure 4.4.1, y-axis). Stocks of black rockfish (CA, WA) and China rockfish (CA) were updated with recent catches, indicating that fishing rates have moved below the overfishing proxy.

Figure 4.4.1 Stock status of groundfish. X-axis: Relative stock status is the ratio of spawning output (in millions of eggs) of the last to the first years in the assessment. Y-axis: Relative fishing intensity is based on stock-specific Spawning Potential Ratios (SPR); plotted values are $(1-SPR)/(1-SPR_{MSY}$ proxy). Horizontal line = fishing intensity rate reference. Vertical lines = biomass target reference point (dashed line) and limit reference point (solid line; left of this line indicates overfished status). Symbols indicate taxonomic group. All points are from the most recent Council-adopted stock assessments.

4.5 HIGHLY MIGRATORY SPECIES

For highly migratory species (HMS), we have been presenting quad plots of recent averages and trends of biomass and recruitment from the most up-to-date stock assessments. These assessments (which range from 2015-2018) have not been updated since last year's ecosystem status report, and thus we have no new information on HMS indicators at this time. Available HMS time series (identical to those in last year's report) are in Appendix I.

4.6 MARINE MAMMALS

Sea lion production: California sea lions are sensitive indicators of prey availability in the central and southern CCE (Melin et al. 2012): sea lion pup count at San Miguel Island relates to prey availability and nutritional status for gestating females from October to June, while pup growth at San Miguel from birth to age 7 months is related to prey availability to lactating females from June to February.
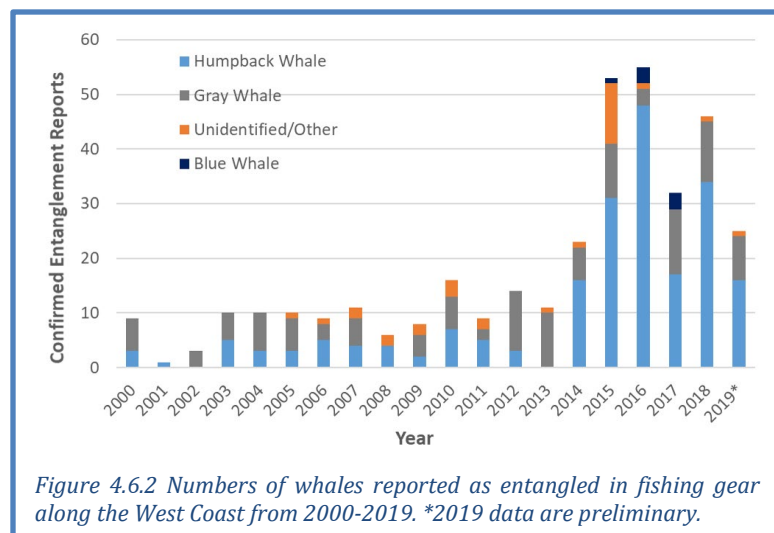
Indicators in Figure 4.6.1 are current through the 2018 pup cohort. These indicators represent the

third consecutive year of average or above average values following 2015, the worst year in the time series. In 2018, pup births were 24% above the long term average and contributed to an increasing trend in pup count over the past 5 years (Figure 4.6.1, top). Pup growth rates were slightly lower than for the 2017 cohort, but were still above the long-term average and supported a short-term increasing trend (Figure 4.6.1, bottom). These improvements coincide with a shift in the nursing female diet. Favorable ocean conditions for anchovy and sardine have resulted in the return of anchovy as the most frequently occurring prey (present in >85% of diets) in the past four years and the resurgence of sardine in the diet in 2018 (48%). Hake, market squid, and Pacific and jack mackerel also had high occurrence in

Figure 4.6.1 California sea lion pup counts, and estimated mean daily growth rate of female pups between 4-7 months on San Miguel Island for the 1997-2018 cohorts. Lines, colors, and symbols are as in Fig. 1.

2018, resulting in a diverse diet of high quality prey for nursing females that likely contributed to the positive trends in the population indices. Preliminary data from the 2019 cohort indicate a 12% decrease in pup count from 2018, which is still above the long-term average. However, pups were in excellent condition through 3 months of age (fall 2019), likely due to the abundance of anchovies supporting nursing adult females; we will provide further updates on the 2019 cohort in our presentation at the March 2020 PFMC meeting.
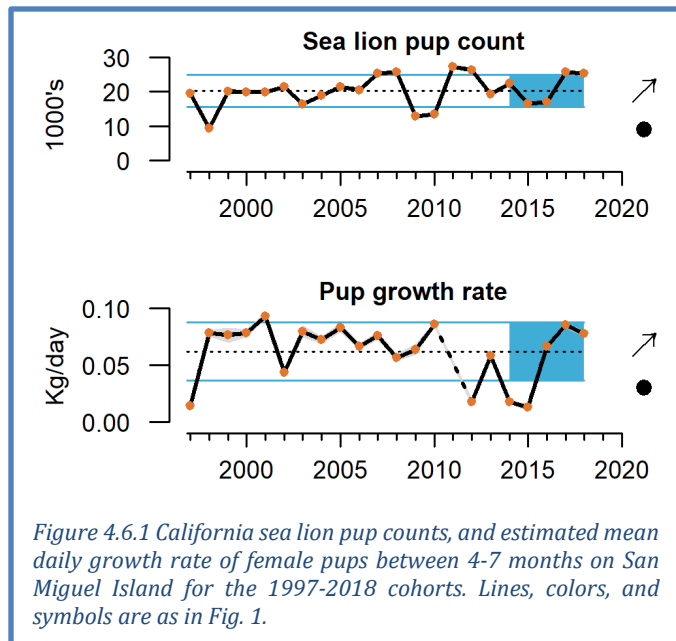
Whale entanglement: The number of whale entanglements reported along the West Coast has increased considerably since 2014, particularly for humpback whales. While ~50% of entanglement reports cannot be attributed to a specific source, Dungeness crab fishing gear is the most common source that has been identified during this period. The dynamics of entanglement risk and reporting are complex, and they are affected by shifts in oceanographic conditions and prey fields, changes in whale populations, changes in distribution and timing of fishing effort, and increased public awareness leading to improved reporting.

In 2019, entanglement reports on the West Coast continued to be higher than prior to 2014, although fewer reports were received than in 2015-2018 (Figure 4.6.2). As in previous years, the majority of reports in 2019 were in California, though entanglements were known to include gear from all three West Coast states and included gear from commercial and recreational Dungeness crab, commercial rock crab, and gillnet fisheries. Significant actions were taken in 2019 to address the increased entanglement reports, including closures and delays of Dungeness crab seasons in California and late-season reductions of allowable

*Figure 4.6.2 Numbers of whales reported as entangled in fishing gear along the West Coast from 2000-2019. *2019 data are preliminary.*

Dungeness crab gear in Washington in response to entanglement risk, and commitments by all three West Coast states to develop conservation plans to reduce entanglements in Dungeness crab fisheries. While these actions likely contributed to reducing entanglement risks in 2019, other factors such as continued exposure of whales to gear that was lost during the season or foraging in nearshore waters on abundant anchovy likely contributed to entanglement risks in 2019.

4.7 SEABIRDS

Seabird indicators (at-sea densities, productivity, diet, and mortality) constitute a portfolio of metrics that reflect population health and condition of seabirds, as well as links to lower trophic levels and other conditions in the CCE. To highlight the status of different seabird guilds and their ecological relationships multiple focal species are monitored throughout the CCE. The species we report on here and in Appendix J represent a breadth of foraging strategies, life histories, and spatial ranges.

Indicators of seabird colony productivity suggested that feeding conditions were patchy in 2019. Fledgling production at colonies in spring 2019 was average to above-average for multiple seabird species at Yaquina Head, Oregon. In contrast, multiple seabird species experienced extremely poor fledgling production off northern and central California (Figure 4.7.1), which reflects the forage patterns in the central CCE reported in Section 4.2. Low availability of krill likely contributed to poor production of Cassin's auklets, which mainly prey on krill. Low availability of juvenile rockfish forced piscivorous birds to prey-switch (Appendix J), which may have led to mismatches; for example, while anchovy were abundant in this region (Figure 4.2.2), they may have been too large for some seabird chicks to ingest.

As further evidence of poor or mismatched prey availability in this region, large numbers of dead, emaciated adult common murres were observed on beaches in northern California during the 2019 breeding season (Appendix J.3). No other large mortality events ("wrecks") of seabirds were observed in late 2018-early 2019 (Appendix J.3). However, unusually high post-breeding mortality of rhinoceros auklets occurred in fall 2019 off Washington and Oregon, suggesting poor feeding conditions in the northern CCE later in the year. Data collection for wrecks in fall/winter 2019-2020 is not complete as of the briefing book deadline, so data from this rhinoceros auklet mortality event are not yet available.
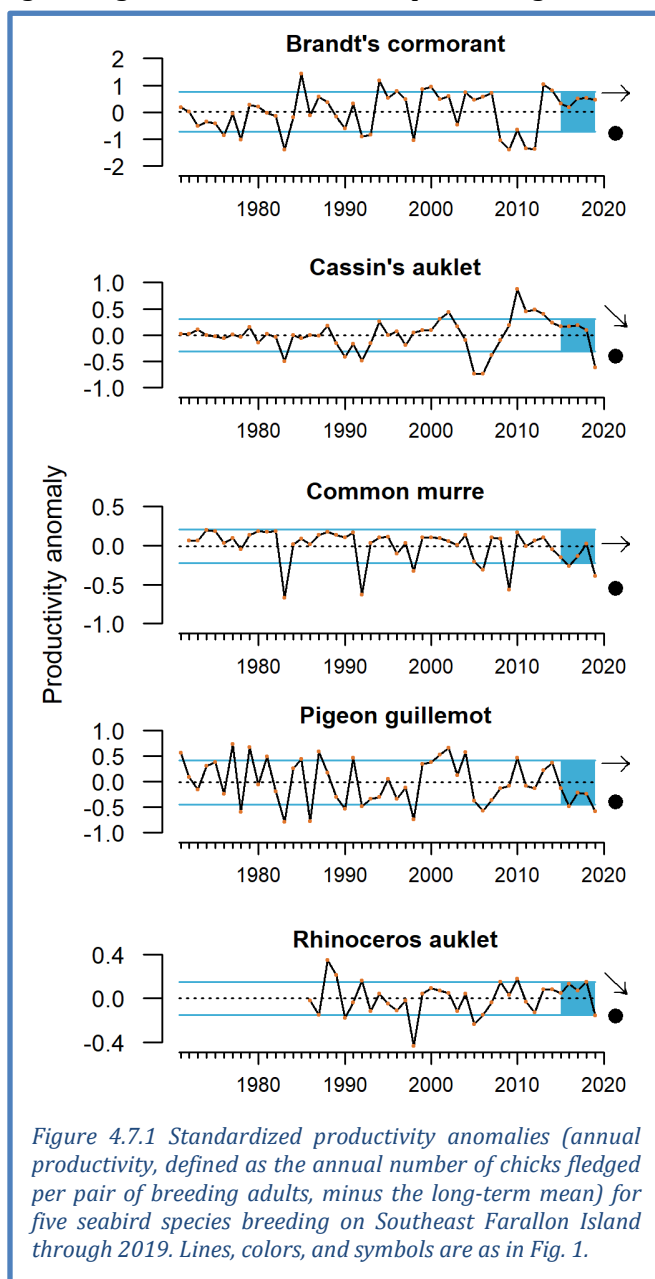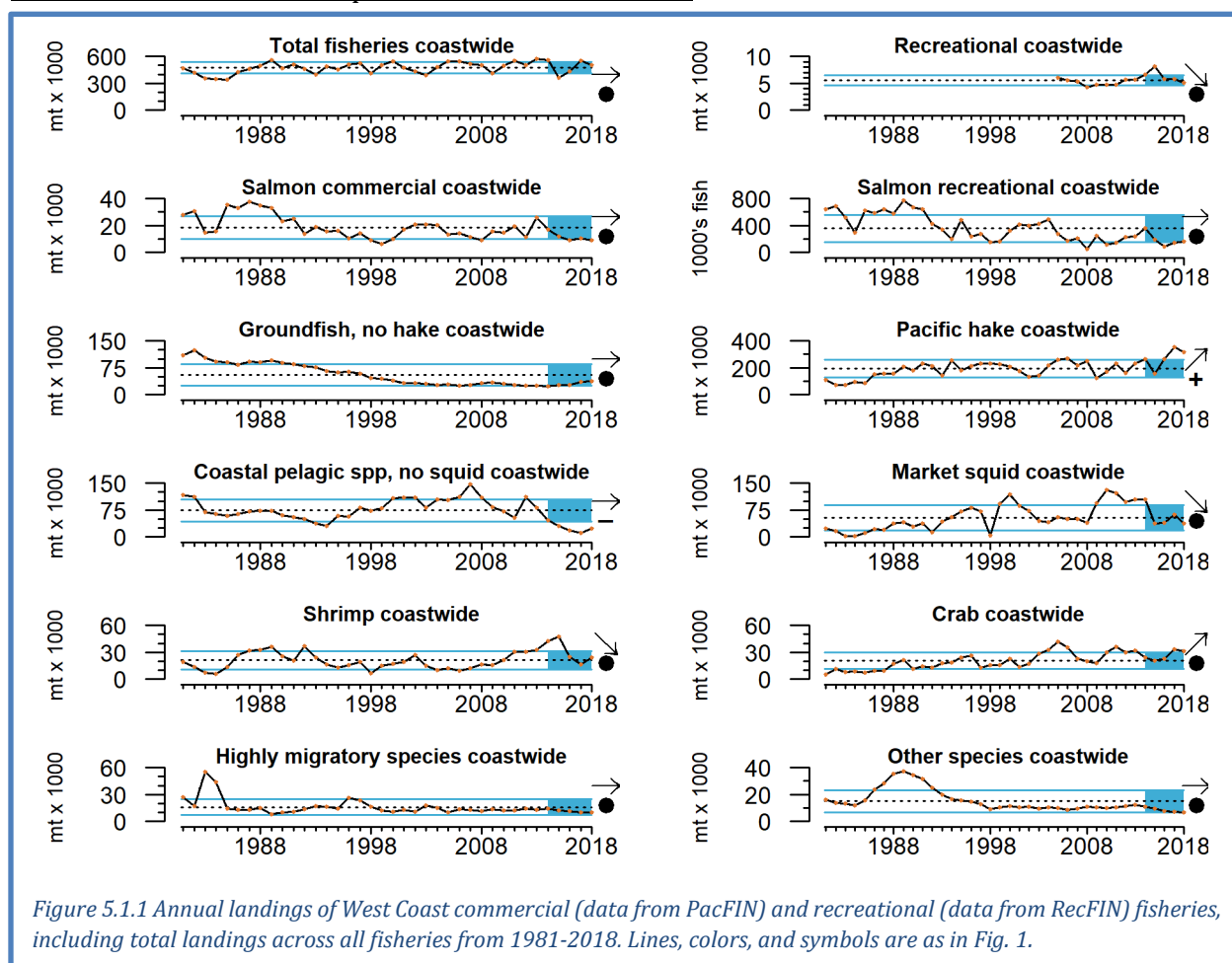

Figure 4.7.1 Standardized productivity anomalies (annual productivity, defined as the annual number of chicks fledged per pair of breeding adults, minus the long-term mean) for five seabird species breeding on Southeast Farallon Island through 2019. Lines, colors, and symbols are as in Fig. 1.

5 HUMAN ACTIVITIES

5.1 COASTWIDE LANDINGS BY MAJOR FISHERIES

Data for fishery landings are complete through 2018. Coastwide landings have been highly variable in recent years, driven by large Pacific hake landings and steep declines in CPS (Figure 5.1.1). Total landings decreased 8% from 2017 to 2018. Pacific hake landings increased to the highest levels of the time series from 2014–2018, and made up 63% of total coastwide landings in 2018. Commercial salmon landings were near the lowest of the time series over the last 5 years. Landings of groundfish (excluding hake) have been low since the mid-2000s, but showed slight increases in 2017 and 2018. Landings of CPS finfish were near the lowest of the time series, and market squid landings have decreased over the last 5 years. Shrimp landings have decreased, while landings of crab have increased over the last 5 years. Landings of HMS and Other species have been consistently within ±1 s.d. of long-term averages over the last 20+ years, although both are near lows for the time series. State-by-state landings are presented in Appendix K. We hope to have updates for 2019 landings by the time of the March 2020 presentation to the Council.

Figure 5.1.1 Annual landings of West Coast commercial (data from PacFIN) and recreational (data from RecFIN) fisheries, including total landings across all fisheries from 1981-2018. Lines, colors, and symbols are as in Fig. 1.

Recreational landings (excluding salmon and Pacific halibut) have decreased over the last 5 years (Figure 5.1.1), due to decreases in yellowfin tuna, yellowtail and lingcod landings in California and decreases in albacore and black rockfish landings in Oregon and Washington. Landings for recreationally caught Chinook and coho salmon showed no trends, but were at consistently low levels from 2014–2018. State-by-state recreational landings are in Appendix K.

Total revenue for West Coast commercial fisheries in 2018 was 7% lower than 2017, due to decreases in market squid, Pacific hake, groundfish and HMS. Revenue was within ± 1 s.d. of time series averages for most fisheries, except for crab (>1 s.d. above average) and CPS finfish (>1 s.d. below average). Shrimp revenue decreased sharply over the last 5 years, though it did increase in 2018 over 2017. Coastwide and state-by-state revenue data are presented in Appendix K.2.

5.2 GEAR CONTACT WITH SEAFLOOR

Benthic species, habitats and communities can be disturbed by natural processes and human activities (e.g., fishing, mining, dredging). The impacts of disturbance likely differ by seafloor type, with hard, mixed and biogenic habitats needing longer to recover than soft sediment. To illustrate spatial variation in bottom trawling activity, we estimated total distance trawled on a 2x2-km grid from 2002-2018. For each grid cell, we mapped the 2018 total distance trawled, the 2018 anomaly from the long-term mean and the most recent 5-year trend.

Off Washington, distance trawled in 2018 was above average and increasing in central waters (Figure 5.2.1 center and right, red cells), while northern and southern cells mostly experienced average or below-average bottom contact; trawl contact was decreasing in southern, nearshore waters (Figure 5.2.1 right, blue cells). Off Oregon, above average bottom contact in 2018 and increasing trends over the last 5 years were observed in several patches, the largest of which were off Central Oregon. Below-average anomalies in 2018 and decreasing trends were most concentrated off southern Oregon. In California, the most notable patches of above average bottom contact in 2018 and increased trawling over the last 5 years were just north of Cape Mendocino, while cells near the California-Oregon border and just north of San Francisco Bay experienced below-average bottom contact in 2018. Further information on methods and coastwide bottom trawl contact trends is available in Appendix L.
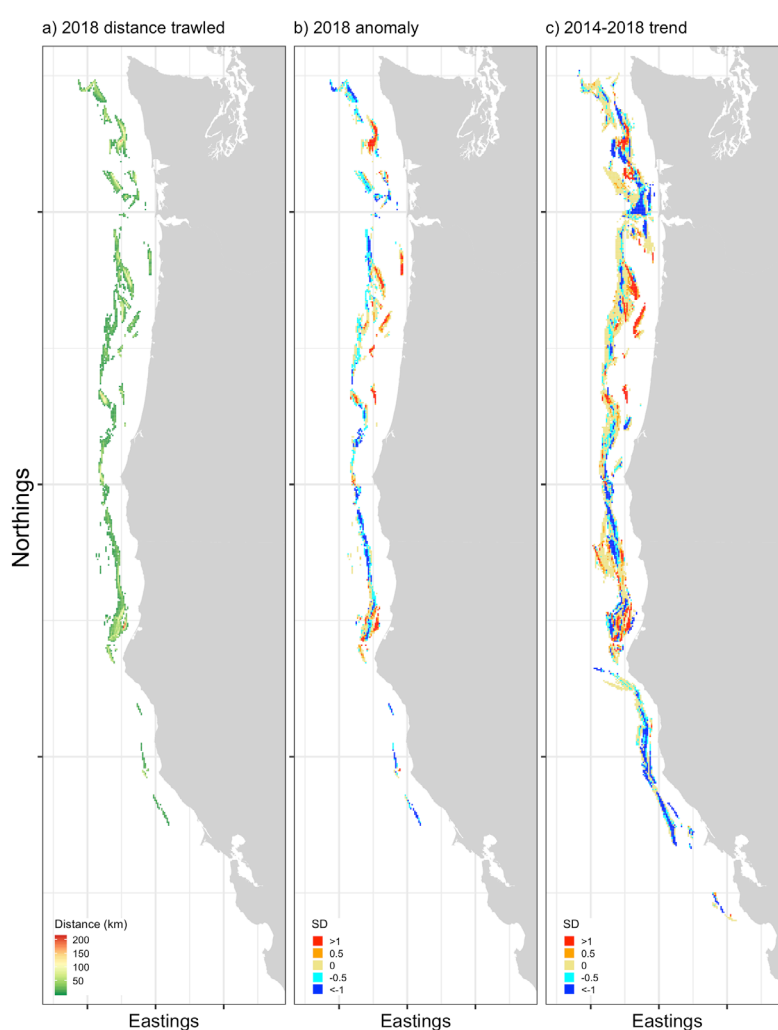

Figure 5.2.1 Analysis of distances trawled using bottom trawl gear in 2x2 km grid cells from 2002–2018. Left: Total distances trawled in 2018. Middle: Anomalies in 2018 relative to the long-term mean. Right: Normalized trend values for the most recent five-year period (2014–2018). Grid cell values >1 (red) or <-1 (blue) represent a cell in which the anomaly or 5-year trend was at least 1 s.d. away from the long-term mean of that cell.
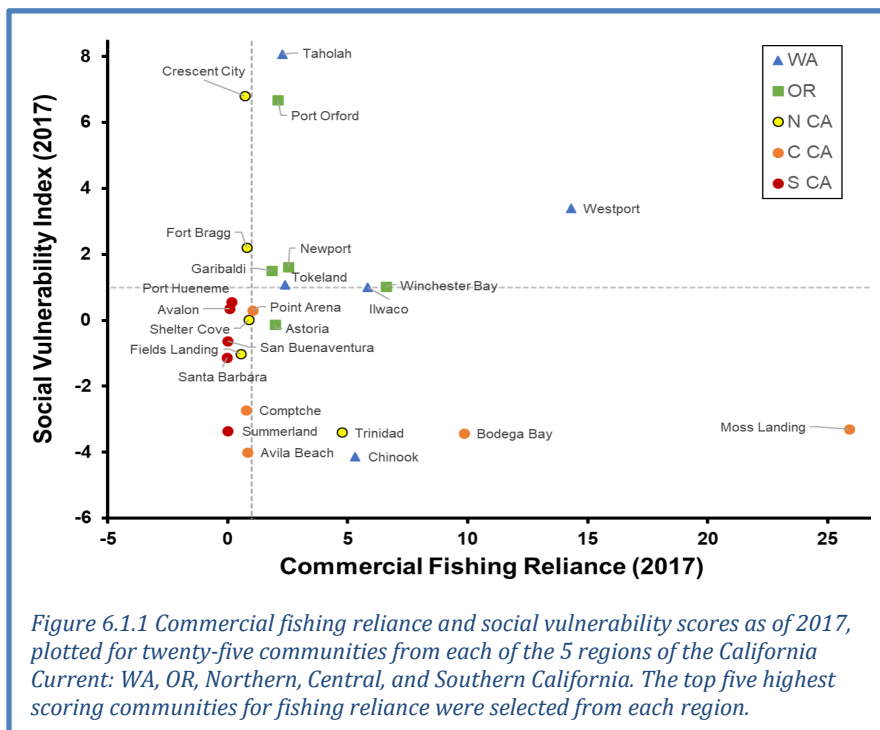
6 HUMAN WELLBEING

6.1 SOCIAL VULNERABILITY

Coastal community vulnerability indices are generalized socioeconomic vulnerability metrics for communities. The Community Social Vulnerability Index (CSVI) is derived from social vulnerability data (demographics, personal disruption, poverty, housing, labor force structure, etc.; Jepson and Colburn 2013). We monitor CSVI in communities that are highly reliant upon fishing.

The commercial fishing reliance index reflects *per capita* engagement in commercial fishing (e.g., landings, revenues, permits, and processing) in 1140 West Coast communities. Figure 6.1.1 plots CSVI updated through 2017 against commercial fishery reliance for communities that are most reliant on commercial fishing along the West Coast. Communities above and to the right of the dashed lines are those with above average levels of CSVI (horizontal dashed line) and commercial fishing reliance (vertical dashed line). For example, Westport and Port Orford have fishing reliance (14.3 and 2.1 s.d. above average, respectively) and high CSVI (3.4 and 6.7 s.d. above average) compared to other coastal fishing communities. Coastal fishing communities that are outliers in both indices may be especially socially vulnerable to downturns in commercial fishing. Additional findings on these relationships are in Appendix M.

Figure 6.1.1 Commercial fishing reliance and social vulnerability scores as of 2017, plotted for twenty-five communities from each of the 5 regions of the California Current: WA, OR, Northern, Central, and Southern California. The top five highest scoring communities for fishing reliance were selected from each region.

In last year's report, we also compared CSVI with recreational fishing reliance, which reflects *per capita* recreational fishing engagement (e.g., number of boat launches, number of charter boat and fishing guide license holders, number of charter boat trips, bait and tackle shops, etc.). Unfortunately, the data used in last year's report were available only through 2016 and have not been updated since; we will have to identify alternate indices of recreational engagement for future reports.

6.2 DIVERSIFICATION OF FISHERY REVENUES

According to the Effective Shannon Index (ESI) that we use to measure diversification of revenues across different fisheries (see Appendix N), the fleet of 28,000 vessels that fished the West Coast and Alaska in 2018 was essentially unchanged from 2017, but was less diverse on average than at any time in the prior 37 years (Figure 6.2.1a). Diversification rates for most categories of vessels fishing on the West Coast have been trending down for several years, but there was little change over the last year for most vessels (Figure 6.2.1b-d). The California fleet had a slight increase in diversification in recent years while diversification of the Washington and Oregon fleets continued to decline. The long-term declines are due both to entry and exit of vessels and changes for individual vessels. Less

19

diversified vessels have been more likely to exit; vessels that remain in the fishery have become less diversified, at least since the mid-1990s; and newer entrants have generally been less diversified than earlier entrants. Within the average trends are wide ranges of diversification levels and strategies, and some vessels remain highly diversified. Additional port-level results are presented in Appendix N.

6.3 REVENUE CONSOLIDATION

At the request of Council advisory bodies, we are working to develop indicators relevant to National Standard 8 (NS-8) of the Magnuson-Stevens Act. NS-8 states that fisheries management measures should "provide for the sustained participation of

Figure 6.2.1 Average diversification for US West Coast and Alaskan fishing vessels with >$5K in average revenues (top left) and for vessels in the 2018 West Coast Fleet with >$5K in average revenues, grouped by state (top right), average gross revenue classes (bottom left) and vessel length classes (bottom right).

[fishing] communities" and "minimize adverse economic impacts on such communities." With guidance from economists in the NOAA IEA network, we chose ex-vessel revenue as a potential indicator of progress toward NS-8.

We plotted port-specific commercial revenue as a proportion of total West Coast commercial revenue over time to see if trends existed. Figure 6.3.1 shows the proportion of total revenue from all commercial fishery landings at the top 16 ports (by revenue) from 1982-2018. While many ports have received fairly stable proportions of total revenue over the long term, some have showed clear increases since the early 1980s (Westport, Newport, Astoria) while others have decreased (Bellingham, San Pedro, Terminal Island). This may indicate some consolidation of total commercial revenue. All ports have experienced interannual variability, of varying magnitude. FMP-specific plots are available in Appendix O.
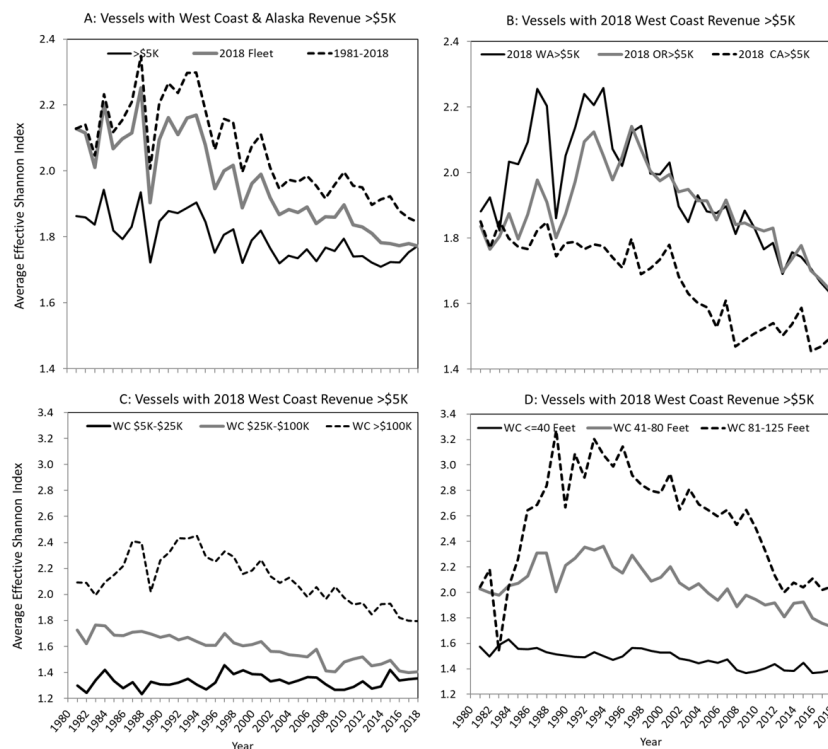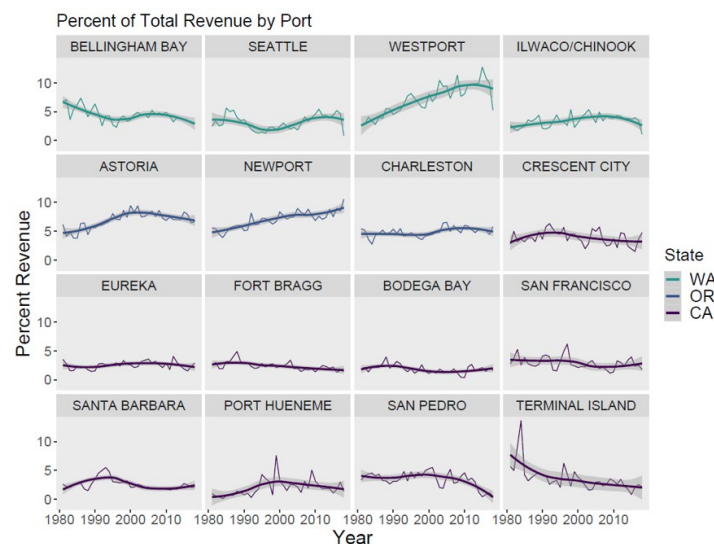

Figure 6.3.1 Port-specific percentages of total commercial fishing revenue, 1982-2018, for the top 16 ports by revenue during this period. Data are based on port-specific revenue share relative to coastwide revenue in a given year. Heavy line is LOESS model fit with 95% confidence interval.

We stress that this analysis is preliminary (see Appendix O), and presented for the purpose of initiating discussion on how to proceed with development of this indicator. We have not attempted to interpret findings with respect to NS-8, or to link changes to specific causes. We will work with the Council and advisory bodies to develop recommendations for further analyses.

7 SYNTHESIS

7.1 SUMMARY OF RECENT CONDITIONS

The CCE was strongly and negatively affected in 2014-2016 by a marine heatwave (the "Blob"), with impacts such as poor productivity, a major HAB event, shifts in species distributions, and lost fishing opportunities. A positive sign was high production of juvenile groundfish, supporting ongoing recovery of many groundfish stocks. In 2017-2018, the system exhibited some recovery from the marine heatwave: physical conditions were largely (but not entirely) similar to long-term averages, and many species showed signs of increased productivity, particularly anchovy. Yet, the system also showed lingering effects from the heatwave, including subsurface heat, high concentrations of pyrosomes, and whale entanglements in fishing gear. Other concerning signs included persistently low NPGO, widespread hypoxia, episodes of north Pacific warming, and loss of fishery diversification.

In 2019, environmental conditions for the CCE were largely consistent with poorer production, including a weak El Niño event in the first half of the year, persistence of the weak NPGO, and a large, surface-oriented marine heatwave in the second half of the year (see Section 7.2). Ecological responses that could possibly be connected to these poor conditions were mostly in northern and central California waters, and included poor production of krill, declines in other forage such as juvenile rockfishes, increases in pyrosomes, and poor production and high mortality at seabird colonies in central and northern California. Ecological indicators off Washington and Oregon (e.g., copepod community composition, juvenile salmon catches, seabird productivity, disappearance of pyrosomes) and Southern California (e.g., anchovy abundance, sea lion pup production) were more favorable, although there is some evidence that the productive season in the northern CCE was truncated in late summer.

7.2 THE 2019 MARINE HEATWAVE: TIMELINE AND "HABITAT COMPRESSION"

We close this year's main report with an assessment of the northeast Pacific marine heatwave that occurred in 2019. We reserved this assessment for the end of the report because the 2019 heatwave occurred later in the year, after many surveys had already been completed. Thus, it is difficult to conclude what ecological and socioeconomic impacts it may have had on the CCE, and we hoped to avoid the perception of direct attribution. However, due to the magnitude of this event, it deserves mention, particularly given the recent history of marine heatwaves in the CCE.

As described in Section 3.1.1, high SST anomalies over large portions of the northeast Pacific in summer and fall of 2019 marked the appearance of a large marine heatwave, similar in many respects to the Blob of 2013-2016. The 2019 event began offshore in late May (Figure 7.2.1, left), and by July 13th the feature intersected coastal Washington (Figure 7.2.1). The feature peaked in size and intensity in August and September 2019, when it reached an area >8 x 10^6 km^2 and an average intensity of >4°C above normal, which rivaled the Blob in size and intensity (Appendix D.2). At that time, the 2019 feature intersected the coast for all of Washington, Oregon and northern California (Figure 7.2.1). After that point, the feature receded from the coast and weakened, thus reducing its potential impacts on the coastal CCE. This continued until by mid January 2020, the feature no longer met the criteria for being a marine heatwave, although SST was still warmer than normal for a large offshore region of the northeast Pacific (Figure 7.2.1, right). Compared to the 2013-2016 event, the 2019 marine heatwave did not penetrate as deeply into the water column. However, there remains a large amount of stored heat in the north Pacific water column following the heatwaves of 2013-2016,
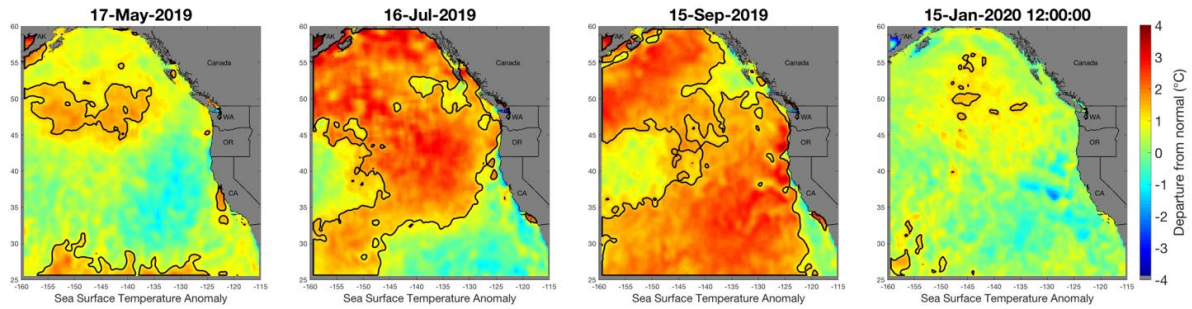
Figure 7.2.2 Standardized SSTa across the Pacific Northeast for May, July, and September 2019, and January 2020. Dark contours denote regions that meet the criteria of a marine heat wave (see text and Appendix D.2). The standardized SSTa is defined as SSTa divided by the standard deviation of SSTa at each location calculated over 1982-2019, thus taking into account spatial variance in the normal fluctuation of SSTa.

2018, and now 2019. Further details on this event, how it compared to the Blob, and our analytical methods are provided in Appendix D.2.

A concept emerging from these warming events is "habitat compression." The large-scale warming in the northeast Pacific over the past 7 years mostly occurred offshore, while much of the nearshore region experienced average temperatures due to upwelling. However, this relatively cool upwelling habitat was restricted to a narrow band along the coast by the warm offshore conditions. This compressed the cool upwelling habitat and consequently altered pelagic species composition and distribution, from forage species to top predators. Habitat compression led to severe impacts such as those associated with whale entanglements in fixed fishing gear, and may have contributed to poor conditions experienced by a number of species off central and northern California in 2019. Santora et al. (2020) developed a Habitat Compression Index (HCI) to track changes in the extent of cold upwelled surface waters, how far that habitat extends offshore, and its latitudinal variability (Figure 7.2.2). The HCI is defined as the area of cool (≤12°C) monthly averaged surface temperatures in a region extending from the coast to 150 km offshore between 35.5°N-40°N (roughly from Morro Bay to Cape Mendocino). Figure 7.2.2 demonstrates the strong shift in compression that occurred in 2014, and has continued since then, especially in winter.

The HCI provides a new regional metric for assessing the impact of warming events on coastal upwelling conditions and should be combined with other marine heatwave diagnostics. Similar levels

Figure 7.2.1 Mean winter (Jan - March) and spring (April - June) habitat compression index (SST < 12C, x100 km²) for 1980-2019. Error envelope indicates ± 1.0 s.e. Lines, colors, and symbols are as in Fig. 1.

of compression have been observed in earlier years (Figure 7.2.2), and we will continue to study this metric in relation to other indicators in hopes of understanding why coastal imp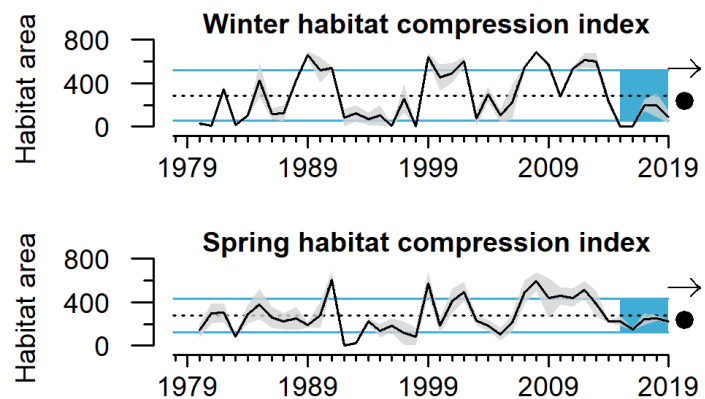acts in recent years have been so severe.